THE UNIVERSITY of EDINBURGH

Edinburgh Research Explorer

Formation processes of dunites and chromitites in Orhaneli and Harmanck ophiolites (NW Turkey): Evidence from in-situ Li isotopes and trace elements in olivine

Citation for published version:
Chen, C, De Hoog, JCM, Su, B, Wang, J, Uysal, I & Xiao, Y 2020, 'Formation processes of dunites and chromitites in Orhaneli and Harmanck ophiolites (NW Turkey): Evidence from in-situ Li isotopes and trace elements in olivine', *Lithos*, pp. 105773. https://doi.org/10.1016/j.lithos.2020.105773

Digital Object Identifier (DOI):
10.1016/j.lithos.2020.105773

Link:
Link to publication record in Edinburgh Research Explorer

Document Version:
Peer reviewed version

Published In:
Lithos

Publisher Rights Statement:
© 2020 Elsevier B.V. .

General rights
Copyright for the publications made accessible via the Edinburgh Research Explorer is retained by the author(s) and / or other copyright owners and it is a condition of accessing these publications that users recognise and abide by the legal requirements associated with these rights.

Take down policy
The University of Edinburgh has made every reasonable effort to ensure that Edinburgh Research Explorer content complies with UK legislation. If you believe that the public display of this file breaches copyright please contact openaccess@ed.ac.uk providing details, and we will remove access to the work immediately and investigate your claim.

OPEN ACCESS

Download date: 05. May. 2023

Elsevier Editorial System(tm) for Lithos
Manuscript Draft

Manuscript Number: LITHOS9129R2

Title: Formation processes of dunites and chromitites in Orhaneli and Harmancık ophiolites (NW Turkey): evidence from in-situ Li isotopes and trace elements in olivine

Article Type: Regular Article

Keywords: olivine; trace element; Li isotopes; ophiolite; chromitite; mantle-crust transition zone

Corresponding Author: Dr. Chen Chen, Ph.D.

Corresponding Author's Institution:

First Author: Chen Chen, Ph.D.

Order of Authors: Chen Chen, Ph.D.; Jan C.M. De Hoog; Ben-Xun Su; Jing Wang; İbrahim Uysal; Yan Xiao

Abstract: Trace elements and Li isotopic compositions of olivine from the mantle-crust transition zone of the Bursa ophiolites (including Orhaneli ophiolite and Harmancık ophiolite) in NW Turkey were measured to constrain the genesis of these dunites and chromitites. A cumulate origin for dunite can be ruled out due to the depletion of incompatible trace elements (Zr, Ti, and heavy rare earth elements) in olivine, instead the chemical signatures point to a replacive origin via melt-rock interaction. The olivine grains in the dunites have lower MnO (0.06-0.15 wt.%), Co (106-137 ppm), Ca (73-323 ppm), and higher NiO (0.23-0.44 wt.%) concentrations than olivine phenocrysts in MORB, suggesting these transition-zone dunites have equilibrated with extremely depleted melts. Additionally, the relatively small δ7Li variations of olivine (average δ7Li +4.8 to +8.7‰) of the Orhaneli suite indicate the Li isotopic compositions of melts percolating through these dunites are relatively homogeneous. However, the large δ7Li variations of olivine (-2.5 to 20.3‰) in Harmancık dunites can be explained by incomplete diffusive equilibration with melts percolating through these dunites, suggesting infiltration happened not long before obduction of the ophiolite. Olivine in chromitites has higher Fo (92.6-94.7) than coexisting dunites, likely induced by subsolidus Mg-Fe exchange between olivine and chromite. The higher chromite contents of the chromitites can also explain the lower concentrations of Sc, V, Co and Zn in coexisting olivine grains. Mixing of depleted mantle-derived melts and boninitic magmas is suggested to induce a compositional shift from the olivine-chromite cotectic line to the liquidus field of chromite, causing the precipitation of chromite and formation of chromitite layers in the dunites. The heavy Li isotopic compositions (+5 to +11‰) of olivine in chromitites and dunites compared to MORB, together with the estimated compositions of parental magmas (Al_2O_3: 9.8-11.4 wt.%; TiO_2: 0.22-0.38 wt.%) for the chromitites, indicate an arc-like geochemical affinity, hence a subduction-related setting in which these mantle-crust transition zones formed.

Research Data Related to this Submission

Title: Data for: Formation processes of dunites and chromitites in Orhaneli and Harmancik ophiolites (NW Turkey): evidence from in-situ Li isotopes and trace elements in olivine
Repository: Mendeley Data
https://data.mendeley.com/datasets/6nwr9d8z78/draft?a=ebf4efdf-b318-4ee5-8fc4-d1d0276533ea

Formation processes of dunites and chromitites in Orhaneli and Harmancık ophiolites (NW Turkey): evidence from in-situ Li isotopes and trace elements in olivine

Chen Chen[1,2,3*], Jan C.M. De Hoog[4*], Ben-Xun Su[1,3,5], Jing Wang[1,3,5], İbrahim Uysal[6], Yan Xiao[3,7]

[1] Key Laboratory of Mineral Resources, Institute of Geology and Geophysics, Chinese Academy of Sciences, Beijing 100029, China

[2] Key Laboratory of Mineralogy and Metallogeny, Guangzhou Institute of Geochemistry, Chinese Academy of Sciences, Guangzhou 510460, China

[3] Innovation Academy for Earth Science, Chinese Academy of Sciences, Beijing 100029, China

[4] Grant Institute, School of GeoSciences, The University of Edinburgh, Edinburgh, EH9 3FE, United Kingdom

[5] University of Chinese Academy of Science, Beijing, 100049, China

[6] Department of Geological Engineering, Karadeniz Technical University, 61080 Trabzon, Turkey

[7] State Key Laboratory of Lithospheric Evolution, Institute of Geology and Geophysics, Chinese Academy of Science, Beijing 100029, China

[*]Corresponding authors: chenchen2@gig.ac.cn (Chen Chen)

ceesjan.dehoog@ed.ac.uk (Jan C.M. De Hoog)

*Revision Notes
Click here to download Revision Notes: revision note.docx

Dear editor,

We really appreciate the insightful comments on our submission by you and the two reviewers, which gave us the opportunity to clarify several important aspects of our manuscript. We revised the manuscript according to the comments, with the major changes as follows:

1. Figure 9 and 12 are modified, and the corresponding explanations are provided in the figure captions. Previous Figure 6 and Figure 10 are removed from the revised version. The related sentences in the text are revised accordingly.

2. The "Highlights" have been shortened.

3. Unrelated references have been removed from the revised version and the total number of references is now 79.

In addition, all editorial comments by the reviewers have been incorporated in the revised version, and point-to-point responses to more detailed comments are listed below. All changes have been highlighted in yellow in the revised manuscript.

We hope you find this revised version of the manuscript suitable for publication in *Lithos*, and look forward to any further comments.

Best regards,
Chen Chen and co-authors

Detailed responses to comments (our responses in red font)

Editor's comments:

Both reviewers find the topic of interest and suggest minor revisions. Based on the two favorable reviews and my own reading of the paper, I am pleased to inform that your paper should be acceptable for publication in the journal after suitable revision is made following the reviewer comments.

1. Highlights 1-3 are too long. Each bullet point of highlights should be no more than 85 characters, including spaces.

Reply: The highlights have been shortened.

2. The number of references exceeds the Lithos maximum of 80. Please reduce the number of references.

Reply: Unrelated references have been removed from the revision and reference number is now 79.

3. Submit data tables 1 to 3 as supplementary material for online publication.

Reply: Data tables 1 to 3 have now been prepared supplementary material for online publication.

Reviewer #1:

The authors have made in-situ analyses on trace element and Li isotopic compositions of olivine from dunites and chromitites in Orhaneli and Harmancik ophiolites (NW Turkey) to unravel the genesis of the host rocks. The data were clearly reported; the manuscript is well structured and fully referenced. Based on the data, the authors made reasonable discussion for the genesis of the dunites and chromitites.

I have only minor comments on the manuscript as shown below:

1. The authors proposed that dunites have equilibrated with the depleted melts as revealed by trace element compositions of olivine in dunites from both Orhaneli and Harmancik ophiolites. But the large <delta>7Li variations among individual samples and the negative correlation between Li concentrations and <delta>7Li values for the Harmancik dunites indicate the incomplete equilibrium of Li isotopes between dunites and incorporated melts shortly before obduction and exhumation. As Li has higher diffusivity than other trace elements in olivine, these observations implicate that they belong to different stages of melt percolation. In the manuscript, I suggest that the authors clarify the temporal and original relationship of percolated melts responsible for the formation of dunites, and the formation of chromitites, and the large <delta>7Li variations among individual samples, respectively.

Reply: Some Templeton experiments found that the isotopic gradients dissipate slower than gradients in the parent element. Richter et al. (2014) reported that very large lithium isotopic fractionations persisted after the lithium concentration had become effectively homogenized during diffusion process, suggesting that it still takes longer for the isotopic composition to become uniform compared to the time it takes for diffusion to homogenize the total lithium concentration. Thus, we can observe the Li element and other trace element concentrations of olivine in dunites from Harmancik ophiolite are equilibrated with the infiltrating melts, whereas the δ^7Li variations of olivine are large, which is caused by incomplete equilibrium of Li isotopes between dunites and incorporated melts. Therefore, these observations are the same stage of melt percolation, and not belong to different stages of melt percolation. In the revision, a detailed discussion has been added to Section 6.4.

2. The authors could identify whether there is any correlation between the concentrations of other trace elements (or other geochemical signatures, e.g., Fo) and Li (or <delta>7Li values) in olivine. It may have some implications for the histories of melt percolation.

Reply: According to the reviewer's suggestion, we plotted the figures of concentrations of other trace/major elements and Li concentrations/δ^7Li values, found there are relatively apparent correlations between Li concentrations/δ^7Li values and Ca concentrations or Ni concentrations of olivine, which is also caused by melt-rock interaction. This conclusion is consistent with this paper. Because the reviewer pointed that the manuscript has many figures and suggested deleting or merging some of them, we do not show these figures in the manuscript.

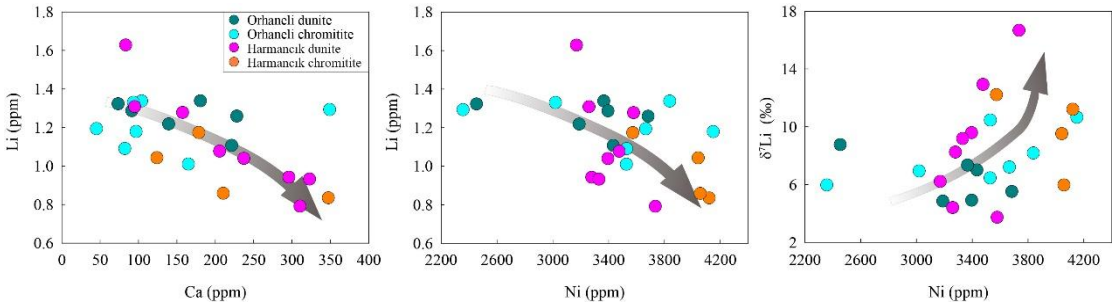

3. The authors ascribed the large heterogeneity of olivine Li isotopic compositions in dunites from the Harmancik ophiolite as the result of disequilibrated Li diffusion during melt percolation. The diffusive addition of Li from melts in short periods can induce relatively higher Li concentrations and lower <delta>7Li values in some samples. However, for samples with heavy Li isotopic compositions (<delta>7Li as high as 20‰), the disequilibrated Li diffusion seems not accountable, as Li concentrations (as low as 0.7 ppm) are markedly lower compared to MORB or IAB (meaning that the diffusive loss of Li from dunites to melts is difficult). In Figure 9, the authors illustrated that these high <delta>7Li values may result from partial melting (inherited from source rocks, depleted peridotites?). For this point, more discussion is needed to make it clear.

Reply: In the olivine of dunite from ophiolites, many studies have reported that there is a negative correlation between Li concentrations and δ^7Li isotopic compositions and the Li concentrations of olivine with high δ^7Li values can be similar to or slightly lower than those in the normal mantle (1.0-1.8 ppm), which can be explained by the interaction between melt and peridotite. For example, in the dunite from Trinity ophiolite, Lundstrom et al. (2015) observed that the δ^7Li values and Li concentrations olivine vary from -5 to 21 ‰ and from 0.6-1.2 ppm, respectively, and Li concentrations vary widely and negatively correlate with δ^7Li for olivines. These features could reflect mineral interaction with hydrothermal fluids where Li partitioning behavior changes with temperature. Su et al. (2016) reported that the olivine in the dunite from the Luobusa ophiolite have Li concentrations (Li isotopic compositions) varying from 0.30 to 0.60 ppm (~10 to 20 ‰). The trend of higher δ^7Li with decreasing Li concentration is also attributed to the diffusion from melts to the surrounding peridotites (Su et al., 2016).

The olivine grains dunites from the Harmancik ophiolite have Li concentrations and Li isotopic compositions varying from 0.7 to 1.9 ppm and from 2.5 to 20.3‰, the ranges and patterns comparable with those in Trinity dunite (Lundstrom et al., 2015), indicating the result of melt-rock interaction process. In the revision, the related discussion has been added to Section 6.4.

Sorry for the confusion, we have deleted the “partial melting” in the Fig. 9.

4. 12 figures in the manuscript are too many for a paper. I suggest deleting or merging some of them. The captions of several important figures are too simple (e.g., Figure 9 and 10). It will be better for understanding if more illustrations are added in

the captions.
Reply: According to the reviewer's suggestion, we have deleted Fig. 6 and Fig. 10 and added detailed description of some important figures.

Reviewer #2:
The paper by Chen et al deals with the formation processes of dunites and chromitites in some Turkish ophiolites via Li isotopes and trace elements in olivine.
The manuscript is well written with only some minor points that should be clarified or added to help the reader.
One of these points is at lines 270-278, where it is written "The chromitites from the two ophiolites display similar Li contents and 7Li values " and then "the data presented here demonstrate that the composition of trace elements and Li isotopes are different". Maybe, the two sentences need some more explanations. They can't be similar and different at the same time.
Reply: Sorry for this confusion. We meant that compared to different δ^7Li compositions of olivine in Orhaneli dunites (3.7 to 11.0‰) and Harmancık dunites (-2.5 to 20.3‰), the δ^7Li compositions of olivine in chromitite from the two ophiolites are similar (5.0 to 14.7‰ in Orhaneli and 4.1 to 15.6‰ in Harmancık). This was clarified in the revision.

It is written that there are good correlations between Mn, Ni and Co but Fig. 7c displaying Co vs Mn shows that for some samples Co values are almost constant while Mn changes, while for some other Mn is constant and Co changes. So, I can't see this good correlation.
Reply: There are good correlations between Ni and Mn, whereas the correlation between Co and Mn is unconspicuous. This description has been modified in the revision.

In fig. 12a it is quite difficult to see the boninitic field. Kamenetsky et al (2001) defined a limit between BON and IAT at about 0.4 wt. % TiO2, while Derbyshire et al (2013 LITHOS) show an overlapping area but in a logarithmic scale it is difficult to see this without some more scale labels.
Reply: According to the figure 10 of Derbyshire et al. (2013), we added the field of boninite in the Fig. 12a, and found our studied samples are plotted in the field of boninite or the nearby IAT field. In the Fig. 12a, we just want to show that the chromite TiO_2 and Al_2O_3 contents plotted directly into the arc field, suggesting the formation of chromite is closely related to the melts from island arc. In the next Fig 12b-c, we further confirmed that the boninite or boninitic melts could be the parental magma of chromite, based on the Cr# of chromite and the calculated composition of melts in equilibrium with chromitite.

In my opinion Fig. 4 is a bit chaotic and difficult to read.
Reply: More detailed descriptions have been added in the captions, so it is clear to read and understand.

In the tables I can't find the values of Mn in ppm but only as wt. %. Did you calculate the ppm values from the wt. % or did you analyzed it by LA-ICP-MS but it was not reported in the tables?
Reply: The values of Mn and Ni in ppm are analyzed by LA-ICP-MS. We have added these values in the Table 3.

There is a diagram with Mg and Fe2+ values for both chromites and olivines but these values are not reported in the tables. Could you, please, add the cation per formula unit of the analyzed minerals.
Reply: We have added the Mg/Fe^{2+} ratios of olivine and chromite to the Table 1 and Table 2, respectively. The MgO and FeO contents of olivine and chromite have been in the Table 1 and Table 2. There is no need to add the Mg and Fe^{2+} values in the tables because the cation Mg and Fe^{2+} is calculated by the MgO and FeO contents of minerals.

Fig. 6 shows Zn vs Co (6a) and Sc vs. Co (6b) of olivine in the dunites and chromitites but in Fig. 6a the scale is 60-160 for Co while it is 250-550 in fig. 6b. I can't understand how it is possible that the range of cobalt is different in the two diagrams. And, however, I'm unable to find a trace element ranging between 250 and 550.
Reply: Sorry for the confusion. The Co contents in the Fig. 6a are the olivine Co contents, while the Co contents in the Fig. 6b are the Co contents of chromite. The Fig. 6 has been deleted in the revision.

Once, Prof Rollinson, author of the book "Using geochemical data", told me that in describing diagram you should say Y vs X so it is MnO vs Fo (Fig. 1) and the same for all the other figures.
Reply: We have modified it in all figure captions.

Other minor points
Line 263: it is written "from 4 to 11" but it seems that the lowest value is 3.7 (OL1 core 5m dunite)
Reply: We modified it.

Line 320: it is written olivine
Reply: We corrected it.

References
Line 56: it is written Pakunc instead of Paktunc
Reply: We corrected it.

Line 713: it should be Jeffcoate with double f
Reply: We modified it.

In the text there are some references that are not present in the reference list such as Zhang et al 2018, Akbulut 2018, Bonavia et al 1993, Ballhaus et al 1991 and Tomascak et al 2000. There is Abily et al 2013 that maybe corresponds to Abily and Ceuleneer 2013, and Tang et al 2009 that could be Tang et al 2011.
The following are written in the reference list but are not cited in the text: Arai and Yurimoto 1994, Coogan et al 2005b, Dick and Bullen 1984, Keleman et al 1992, Richter et al 2014, Su et al 2017, Uysal et al 2009, Xiao et al 2017.
In the text there are two papers by Rospabè et al, one is 2018, the other 2019. In the reference list both are 2018. Check.
Reply: We have checked the references in the text and the references in the reference list, deleted the references which are not cited, added the references which are not present in the reference list but in the text, and confirmed that the references in the text and reference list are same.

*Abstract
Click here to download Abstract: Abstract.docx

Trace elements and Li isotopic compositions of olivine from the mantle-crust transition zone of the Bursa ophiolites (including Orhaneli ophiolite and Harmancık ophiolite) in NW Turkey were measured to constrain the genesis of these dunites and chromitites. A cumulate origin for dunite can be ruled out due to the depletion of incompatible trace elements (Zr, Ti, and heavy rare earth elements) in olivine, instead the chemical signatures point to a replacive origin via melt-rock interaction. The olivine grains in the dunites have lower MnO (0.06-0.15 wt.%), Co (106-137 ppm), Ca (73-323 ppm), and higher NiO (0.23-0.44 wt.%) concentrations than olivine phenocrysts in MORB, suggesting these transition-zone dunites have equilibrated with extremely depleted melts. Additionally, the relatively small δ^7Li variations of olivine (average δ^7Li +4.8 to +8.7‰) of the Orhaneli suite indicate the Li isotopic compositions of melts percolating through these dunites are relatively homogeneous. However, the large δ^7Li variations of olivine (-2.5 to 20.3‰) in Harmancık dunites can be explained by incomplete diffusive equilibration with melts percolating through these dunites, suggesting infiltration happened not long before obduction of the ophiolite. Olivine in chromitites has higher Fo (92.6-94.7) than coexisting dunites, likely induced by subsolidus Mg-Fe exchange between olivine and chromite. The higher chromite contents of the chromitites can also explain the lower concentrations of Sc, V, Co and Zn in coexisting olivine grains. Mixing of depleted mantle-derived melts and boninitic magmas is suggested to induce a compositional shift from the olivine-chromite cotectic line to the liquidus field of chromite, causing the precipitation of chromite and formation of chromitite layers in the dunites. The heavy Li isotopic compositions (+5 to +11‰) of olivine in chromitites and dunites compared to MORB, together with the estimated compositions of parental magmas (Al_2O_3: 9.8-11.4 wt.%; TiO_2: 0.22-0.38 wt.%) for the chromitites, indicate an arc-like geochemical affinity, hence a subduction-related setting in which these mantle-crust transition zones formed.

(1) δ^7Li study of Orhaneli-Harmancık mantle-crust transition zone dunite and chromitite

(2) Orhaneli dunite formed by interaction of peridotite with homogeneous melt batches

(3) Harmancık dunite reflects incomplete diffusive equilibration during melt percolation

(4) Parental magmas of the chromitites show boninitic geochemical affinities.

*Revised Manuscript with No changes marked
Click here to download Revised Manuscript with No changes marked: manuscript with no changes.docx

Formation processes of dunites and chromitites in Orhaneli and Harmancık ophiolites (NW Turkey): evidence from in-situ Li isotopes and trace elements in olivine

Chen Chen[1,2,3*], Jan C.M. De Hoog[4*], Ben-Xun Su[1,3,5], Jing Wang[1,3,5], İbrahim Uysal[6], Yan Xiao[3,7]

[1] Key Laboratory of Mineral Resources, Institute of Geology and Geophysics, Chinese Academy of Sciences, Beijing 100029, China

[2] Key Laboratory of Mineralogy and Metallogeny, Guangzhou Institute of Geochemistry, Chinese Academy of Sciences, Guangzhou 510460, China

[3] Innovation Academy for Earth Science, Chinese Academy of Sciences, Beijing 100029, China

[4] Grant Institute, School of GeoSciences, The University of Edinburgh, Edinburgh, EH9 3FE, United Kingdom

[5] University of Chinese Academy of Science, Beijing, 100049, China

[6] Department of Geological Engineering, Karadeniz Technical University, 61080 Trabzon, Turkey

[7] State Key Laboratory of Lithospheric Evolution, Institute of Geology and Geophysics, Chinese Academy of Science, Beijing 100029, China

[*]Corresponding authors: chenchen2@gig.ac.cn (Chen Chen)

ceesjan.dehoog@ed.ac.uk (Jan C.M. De Hoog)

Abstract

Trace elements and Li isotopic compositions of olivine from the mantle-crust transition zone of the Bursa ophiolites (including Orhaneli ophiolite and Harmancık ophiolite) in NW Turkey were measured to constrain the genesis of these dunites and chromitites. A cumulate origin for dunite can be ruled out due to the depletion of incompatible trace elements (Zr, Ti, and heavy rare earth elements) in olivine, instead the chemical signatures point to a replacive origin via melt-rock interaction. The olivine grains in the dunites have lower MnO (0.06-0.15 wt.%), Co (106-137 ppm), and higher NiO (0.23-0.44 wt.%) concentrations than olivine phenocrysts in MORB, suggesting these transition-zone dunites have equilibrated with extremely depleted melts. Additionally, the relatively small δ^7Li variations of olivine (average δ^7Li +4.8 to +8.7‰) of the Orhaneli suite indicate the Li isotopic compositions of melts percolating through these dunites are relatively homogeneous. However, the large δ^7Li variations of olivine (-2.5 to 20.3‰) in Harmancık dunites can be explained by incomplete diffusive equilibration with melts percolating through these dunites, suggesting infiltration happened not long before obduction of the ophiolite. Olivine in chromitites has higher Fo (92.6-94.7) than coexisting dunites, likely induced by subsolidus Mg-Fe exchange between olivine and chromite. The higher chromite contents of the chromitites can also explain the lower concentrations of Sc, V, Co and Zn in coexisting olivine grains. Mixing of depleted mantle-derived melts and boninitic magmas is suggested to induce a compositional shift from the olivine-chromite cotectic line to the liquidus field of chromite, causing the precipitation of chromite

and formation of chromitite layers in the dunites. The heavy Li isotopic compositions (+6 to +11‰) of olivine in chromitites compared to MORB, together with the estimated compositions of parental magmas (Al_2O_3: 9.8-11.4 wt.%; TiO_2: 0.22-0.38 wt.%) for the chromitites, indicate an arc-like geochemical affinity, hence a subduction-related setting in which these mantle-crust transition zones formed.

Key words: olivine; trace element; Li isotopes; ophiolite; chromitite; mantle-crust transition zone

1. Introduction

The mantle-crust transition zone is well documented in many ophiolites, and marks the petrological transition from mantle peridotites to lower crustal cumulates (e.g., Zhang et al., 2017; Rollinson, et al., 2018; Rospabé et al., 2018). Ophiolitic mantle-crust transition zones typically consist of dunite-dominated ultramafic rocks and stratiform-like chromitites, and can reach a thickness of several kilometers (Paktunc, 1990). These dunites are made of mostly olivine with minor chromite and their thickness ranges from a few meters to a few hundred meters (e.g., Zhang et al., 2017). Although the transition zone chromitites are distinguished by their layered morphology from the mantle podiform chromitites which occur as irregular lenses and pods, their compositions are similar in many cases (e.g., Arai et al., 2004; Rollinson, 2008). Despite many years of investigation, the genesis of the dunites and chromitites in the ophiolitic mantle-crust transition zone is still debated, and different models have been proposed, such as magmatic cumulates stagnating at the base of the crust

(e.g., Abily and Ceuleneer, 2013), crustal assimilation (Arai et al., 2004), reactions between melts and mantle harzburgites (e.g., Abily and Ceuleneer, 2013), and mixing of mantle-derived melts with differentiated magmas (e.g., Ballhaus, 1998). In addition, the nature of the mixed or infiltrated melts and their influences on the mantle-crust transition zone are not yet well known, limiting our understanding of the evolution of ophiolites. A close link between subduction initiation and chromitite/ophiolite genesis has been documented (e.g., Reagan et al., 2017; Zhang et al., 2017) in several studies of the extensive ophiolites in Turkey (e.g., Uysal et al., 2017; Chen et al., 2019). Therefore, careful study of the formation processes of the chromitite and their tectonic setting could shine further light on the relationship between subduction initiation and ophiolite emplacement.

Olivine is a ubiquitous mineral in both the ultramafic and mafic igneous rocks, and in most cases, it is the first silicate phase to crystallize from ultramafic-mafic melts (Foley et al., 2013). Olivine thus controls early magmatic differentiation processes, but its Fo content can provide little information about its origin and evolution (De Hoog et al., 2010; Foley et al., 2013), which forces us to focus on its trace element geochemistry. Consequently, it has become increasingly important to improve our knowledge of the trace element composition of olivine, and to test the use of its geochemical signature as a tracer of early igneous and mantle melting processes (Foley et al., 2013; Rampone et al., 2016). Several studies have shown that olivines in peridotites from different tectonic environments and/or various origins exhibit distinct geochemical characteristics and define systematic elemental

correlations for a series of trace elements (Ni, Mn, Zn, Co, Zr and heavy rare earth elements (HREE)), recording different magmatic processes (Sobolev et al., 2007; De Hoog et al., 2010; Foley et al., 2013; Rampone et al., 2016). Recent work on the Purang and Luobusa ophiolites (Su et al., 2019) advocates that the incompatible trace elements of olivine are more sensitive to melting processes, whereas the concentrations of compatible trace elements are mostly constrained by their source composition.

Lithium and its isotopes (^{6}Li and ^{7}Li) are increasingly used to trace multiple high-temperature processes due to their moderate incompatibility, strong fluid mobility, and large mass difference (17%) between its two isotopes (e.g., Tomascak et al., 2016). Olivine is the dominant Li reservoir in the upper mantle (Seitz and Woodland, 2000; De Hoog et al., 2010), and olivine-melt partition coefficients of Li are virtually independent of pressure, temperature and olivine composition (Seitz and Woodland, 2000; Qian et al., 2010). The equilibrium fractionation of Li isotopes is likely to be negligible at high temperatures (Vlastelic et al., 2009). However, many natural peridotites display heterogeneous δ^{7}Li compositions, which has been attributed to Li diffusion or interaction between percolating melts and peridotites (e.g., Lundstrom et al., 2005; Rudnick and Ionov, 2007; Su et al., 2014). Thus, olivine Li isotopic systematics can be used to trace magmatic processes of mantle-crust transition zone dunites and chromitites.

In the Bursa ophiolites (Orhaneli and Harmancık ophiolites) in northwestern Turkey, mantle-crust transition zones typically contain interlayered dunites and

chromitites (Uysal et al., 2015), the successions of which can reach up a few kilometers thick. In this paper, we provide in-situ trace element and Li isotope analyses of olivine in the chromitites and dunites from the mantle-crust transition zones of Orhaneli and Harmancık ophiolites. These datasets, together with petrological investigations and mineral major oxide compositions, are used to constrain the magmatic processes involved in the formation of dunites and chromitites in ophiolitic mantle-crust transition zones.

2. Geological Setting

Tethyan ophiolites in Anatolia occur in several E-W trending belts, which are separated by a series of Gondwana-derived continental fragments (e.g., Uysal et al., 2014) (Fig. 1a). The Izmir-Ankara Suture Zone (IASZ) in northern Turkey occurs between the Sakarya Zone (continent) to the north and the Anatolide-Tauride continental block to the south (Fig. 1a), and has relatively intact ophiolite blocks, which are locally extensive and well preserved (Dilek and Thy, 2006). The Orhaneli and the Harmancık ophiolites, situated in the western part of the IASZ, are considered as remnants of the Izmir-Ankara-Erzincan ocean, a local term for the northern branch of the Neotethys ocean (Sarıfakıoğlu et al., 2009). The Orhaneli ophiolite was tectonically emplaced onto northwestern Anatolia along the IASZ (Fig. 1a). The Harmancık ophiolite is located ca. 30 km south of the Orhaneli ophiolite (Fig. 1b) (Sarıfakıoğlu et al., 2009). These two ophiolites were thrusted southwards over the metamorphic basement rocks of the Tavşanlı zone in the Anatolide-Tauride platform

133 (Sarıfakıoğlu et al., 2017).

134 The Orhaneli ophiolite is approximately 50 km long, 15 km wide and 1500 m
135 thick (Fig. 1b; Sarifakioglu et al., 2009), and mainly consists of mantle-crust
136 transition zone comprising mostly basal ultramafic cumulates. The transition zone is
137 dominated by chromitite interlayered dunites, followed by wehrlites, lherzolites,
138 harzburgites and pyroxenites and to a lesser extent mafic cumulates such as gabbros
139 and gabbronorites (e.g., Sarıfakıoğlu et al., 2009; Uysal et al., 2015). The chromitites
140 interlayer with dunite in the two ophiolites and have typically semi-massive and
141 banded (stratiform, cumulate) structures (Fig. 2). The mantle-crust transition zone of
142 the Harmancık ophiolite, which reachs up to 1000 m thickness, has similar rock
143 assemblages to those of the Orhaneli ophiolite (Tankut, 1980). The Harmancık
144 ophiolite contains additional podiform chromitites in its mantle section (Sarıfakıoğlu
145 et al., 2009). The podiform chromitites form centimeters to meters scale
146 lenticular/tabular orebodies enclosed in thick dunite envelopes within mantle
147 harzburgites. The mantle harzburgites and dunites from Harmancık ophiolite have
148 been almost completely altered to serpentine and talc, and are unconformably overlain
149 by Neogene sedimentary units (e.g., Uysal et al., 2014, 2015).

150

151 **3. Petrography of dunites and chromitites**

152 In the Orhaneli ophiolite, dunites display adcumulate textures and consist of
153 mostly medium- to fine-grained olivine crystals with minor chromites (Fig. 3a, b).
154 Chromitites generally show adcumulus- to orthocumulus-like textures with euhedral

to subhedral chromite grains (Fig. 3c). They occur as bands and layers in dunites (Fig. 2a-c), and massive chromitites are very rare. The banded chromitite orebodies display schlieren textures, characterized by parallel layers of chromitite alternating with dunite (Fig. 2b). The thickness of the chromitite bands in the Orhaneli ophiolite typically ranges between 0.2 and 3 cm, rarely reaching up to 5 cm (Fig. 2b-c). In contrast, chromitites from the Harmancık mantle-crust transition zone occur as schlieren/bands, semi-massive, and disseminated textures. Chromite grains are mostly euhedral to subhedral. Dunites are made up predominantly of olivine (> 95%) and have a dominant cataclastic texture (Fig. 3d).

In the Orhaneli ophiolite, the mantle-crust transition zone is nearly horizontal (Fig. 2a), and we have selected 13 samples (dunites and chromitites) from the mantle-crust transition zone profile. The thickness of this profile is about 90 m and we fixed the base of the dunite as 0 m and its roof is +90 m. In the Harmancık ophiolite, 12 drill hole samples from the mantle-crust transition zone were selected for chemical analyses, owing to their pristine olivine grains. The drill hole samples including dunite and chromitite were collected from depths of 63.4 m to 73.4 m.

4. Analytical methods

4.1 Major oxide analysis of minerals

Major oxide compositions of olivine and chromite were determined by wavelength-dispersive X-ray spectrometry using a JEOL JXA8100 electron probe micro-analyzer at the Institute of Geology and Geophysics, Chinese Academy of

Sciences (IGGCAS). The analyses were carried out using an accelerating voltage of 15 kV, a 10 nA beam current, a 5 μm spot size and 10-30 s peak counting time. Natural and synthetic mineral standards were used for calibration. A ZAF procedure was used for matrix corrections. Typical analytical uncertainty for the analyzed elements was better than 1.5% (1RSD%).

4.2 Trace element analysis of olivine

In-situ trace element analyses of olivine were conducted on thin sections using a laser ablation inductively coupled plasma mass spectrometer (LA-ICP-MS) at IGGCAS. The LA-ICP-MS system consists of a 193 nm Coherent COMPex Pro ArF Excimer laser coupled to an Agilent 7500a ICP-MS. About 6-8 spots were measured for different olivine grains in each sample. The laser spot size was 140 μm, and the repetition rate was 8 Hz. Each analysis consisted of 60 s measurement of gas blank and 60 s ablation. The following isotopes were measured: ^{7}Li, ^{27}Al, ^{29}Si, ^{31}P, ^{39}K, ^{43}Ca, ^{45}Sc, ^{49}Ti, ^{51}V, ^{53}Cr, ^{59}Co, ^{66}Zn, ^{91}Zr, ^{163}Dy, ^{166}Er, ^{172}Yb. De Hoog et al. (2010) reported that potential interferences in olivine from matrix components MgO, SiO_2 and FeO, which are generated during ablation only and therefore unaccounted for by gas blank subtraction. The contribution of ^{26}Mg^{40}Ar to the ^{66}Zn signal is about 0.2 ppm, and the ^{29}Si^{16}O interference on ^{45}Sc accounted for 0.2 ppm of the signal (De Hoog et al., 2010), hence those are small enough to be ignored. A glass standard, NIST 610, was used for external calibration. For most of the trace elements NIST 612 standard was used to monitor instrument drift, and silicon (^{29}Si) was selected as an internal standard. The SiO_2 contents of NIST 610 and NIST 612 are 69.7% and 72.1%,

199 respectively. Reference values of NIST 610 and NIST 612 are from GeoREM
200 (http://georem.mpch-mainz.gwdg.de). The data were reduced using the GLITTER 4.0
201 program.

202 **4.3 Li concentration and isotope analyses of olivine**

203 In-situ analyses of Li concentrations and isotopic ratios of olivine were carried
204 out on gold-coated polished thin-sections using a Cameca IMS 1270 SIMS at the
205 Edinburgh Ion Microprobe Facility, in the University of Edinburgh, United Kingdom.
206 A $^{16}O_{2-}$ primary ion beam with an intensity of 12-16 nA was accelerated to 22.5 kV
207 and impacted onto the sample surface using Kohler illumination. The elliptical spot
208 area was approximately 20 × 30 μm. The secondary ion beam position in the field
209 aperture and the ^{7}Li peak position were automatically centered before each
210 measurement during a 60-s pre-sputter without beam rastering. Secondary ions were
211 counted in mono-collection, pulse-counting mode. Fifty cycles were measured with
212 counting times of 6 and 2.5 s for ^{6}Li and ^{7}Li, respectively. The count rate for ^{7}Li
213 ranged from 30,000 to 120,000 cps, depending on the Li concentration of the sample
214 and primary beam intensity, resulting in 1 s uncertainties of δ^{7}Li of 0.5-1.2‰.
215 Lithium concentrations were calculated using beam current corrected ^{7}Li count rates
216 of samples using 06JY34Ol as a standard (Li concentration = 1.73 ppm; Su et al.,
217 2015). The Li isotopic ratios are expressed as δ^{7}Li relative to the NIST L-SVEC
218 standard $\{\delta^{7}Li = [(^{7}Li/^{6}Li)_{sample}/(^{7}Li/^{6}Li)_{L\text{-}SVEC} - 1] \times 1000\}$. Basaltic standards
219 BCR2-G and ML3B-G were analyzed to monitor instrument drift, whereas 06JY34Ol
220 (δ^{7}Li = 3.1‰; Su et al., 2015) was used for calibration. Matrix composition (Fo

content) has an effect on measured olivine Li isotopic compositions; e.g., Su et al. (2015) showed that δ^7Li values increase by 1.0‰ for each mole percent decrease in the Fo content of olivine, and this was taken into account for calibration. As Fo contents of the olivines span a narrow range from 91.6 to 94.7, the matrix correction amounted to no more than 3‰, compared to a range of > 20‰ in δ^7Li for the whole dataset.

5. Results

5.1 Major oxide contents of minerals

Olivine in the Orhaneli and Harmancık dunites has Fo values of 92.4-94.0 and 91.6-93.5, respectively (Table S1; Fig. 4a-c). The chromitites contain olivine with somewhat higher Fo values (92.6-94.7 in Orhaneli; 93.3-94.4 in Harmancık) than those in the dunites (Table S1). The dunites from the two ophiolites have similar MnO (0.06-0.15 wt.%) and NiO (0.23-0.44 wt.%) contents in their olivine (Table S1). In the Orhaneli and Harmancık profile analyses, the variations of Mn concentrations in olivines are not continuous and yield abrupt change at the contact with chromitite layers. Compared to Mn, Ni concentrations show the reverse patterns (Fig. 5).

Chromite grains in dunites of the both ophiolites are generally uniform in TiO_2 contents (0.14-0.23 wt.% in Orhaneli; 0.11-0.22 wt.% in Harmancık), similar to those in the chromitites (0.14-0.26 wt.% and 0.13-0.22 wt.%), whereas their Cr# (100 × Cr/(Cr+Al)) and Mg# (100 × Mg/(Mg+Fe)) values are variable within ranges of 79.1-81.8 and 47.6-53.5 in the Orhaneli dunites, 70.6-80.2 and 41.9-52.9 in the

243 Harmancık dunites, 81.1-82.8 and 58.7-67.3 in the Orhaneli chromitites and 78.8-80.0
244 and 46.4-64.2 in the Harmancık chromitites (Table S2; Fig. 4).

245 **5.2 Trace element compositions of olivine**

246 From base to top, the mantle-crust transition zone in the Orhaneli ophiolite
247 includes many cyclic dunite and chromitite layers (Fig. 2a-b) with a total thickness of
248 90 m. Overall, olivines in chromitites show lower Co, Zn, Sc and V concentrations
249 than those in dunites (Fig. 5a, b). The Co concentrations of olivine in the dunites
250 (106-132 ppm in Orhaneli, 128-137 ppm in Harmancık) are higher than those of
251 primitive mantle (105 ppm; McDonough and Sun, 1995), whereas the concentrations
252 of Zn (6.0-44.8 ppm), Sc (2.14-3.68 ppm) and V (0.07-0.36 ppm) in all samples are
253 lower than primitive mantle (Zn: 55 ppm; Sc: 16.2 ppm; V: 82 ppm; McDonough and
254 Sun, 1995). The olivine in both dunites and chromitites from the two ophiolites has
255 lower incompatible trace element concentrations (Ti = 4.0-7.8 ppm, Zr = 0.010-0.034
256 ppm, and Yb = 0.007-0.027 ppm) than the counterparts in olivine phenocrysts in
257 MORB (Table S3; Fig. 6) (e.g., Piccardo et al., 2007; Foley et al., 2011). In the
258 Orhaneli section and Harmancık drill hole samples, there is no apparent correlation
259 between trace element compositions of olivine and the relative position of the layers
260 (Figs. 5, 6).

261 **5.3 Li concentrations and isotopic compositions**

262 In the Orhaneli dunites, olivine has Li concentrations varying from 0.9 to 1.5
263 ppm, and δ^7Li from 3.7 to 11.0‰ (Fig. 7), with no correlation between Li
264 concentrations and Li isotopic compositions (Fig. 8). In contrast, Li concentrations

(0.7 to 1.9 ppm) and δ^7Li values (-2.5 to 20.3‰) of olivine in the Harmancık dunites vary widely (Table S1), and the δ^7Li values are negatively correlated with the Li concentrations (Fig. 8). Most olivine grains in the two ophiolites show little change in Li concentrations and δ^7Li values from core to rim (Table S1). Nevertheless, different olivine grains in the same sample from Harmancık can have strongly variable Li isotopic compositions (up to 15‰ difference) (Table S1; Fig. 7). On the other hand, the chromitites from the two ophiolites display Li contents and δ^7Li values of olivine with 0.8 to 1.6 ppm and 5.0 to 14.7‰ in Orhaneli and 0.7 to 1.2 ppm and 4.1 to 15.6‰ in Harmancık (Table S1; Fig. 7).

6. Discussion

Based on trace elements and Li isotopes compositions of olivine in the dunites and chromitites from the mantle-crust transition zones for both ophiolites, we first evaluate the various processes that may account for the observed trace elemental and Li isotope variations, followed by models for the formation of dunites and chromitites.

6.1 Origin of mantle-crust transition zone dunites in the Orhaneli and Harmancık ophiolites

Dunite consists almost entirely of olivine and is usually formed by one of three processes (e.g., Su et al., 2016; Yao et al., 2018): 1) ultrahigh-degree partial melting of mantle with nearly all orthopyroxene being exhausted; 2) cumulate dunite left behind by the fractionation and accumulation of abundant olivine from an ultramafic-mafic

287 magma; 3) reaction between silica-undersaturated melt migrating in channels and
288 pyroxene-rich wall rock triggering the formation of replacive dunite.

289 Cumulate dunites are formed via crystal accumulation from magmas and
290 therefore olivine generally has low Fo (88-91) and feature a rapid decrease in the NiO
291 content with decreasing Fo (Santos et al., 2002; Song et al., 2007; Arai et al., 2012;
292 Seo et al., 2013; Su et al., 2016; Rospabé et al., 2018). Moreover, the coexisting
293 chromites show a wide range of Cr# from 15 to 76 as well as high TiO_2 contents (up
294 to 0.8 wt.%) (Santos et al., 2002; Song et al., 2007; Arai et al., 2012; Seo et al., 2013)
295 (Fig. 4a-c). In contrast, olivine in replacive dunites generally has higher Fo values (up
296 to 94), because the high-MgO melts reacting with peridotites convert olivine and
297 pyroxene in peridotite to high-Fo olivine (Rollinson et al., 2018). Besides, no obvious
298 correlation exists between the Fo and NiO of olivine grains within the replacive
299 dunites (Mazzucchelli et al., 2009). In the Orhaneli and Harmancık dunites, olivine
300 has higher Fo (91.6-94.0) and lower MnO contents (0.06-0.15 wt.%) than that from
301 cumulate dunites, while chromites display higher Cr# (79.1-82.8) and lower TiO_2
302 contents (0.14-0.26 wt.%) (Fig. 4c-d). These observations, together with the absence
303 of a clear correlation between Fo and NiO in olivine, demonstrate that the dunites
304 from both ophiolites could not be related to fractional crystallization (Fig. 4b). Instead,
305 all our data fall within the fields of replacive dunites (Fo: 90.4-94.6; MnO of olivine:
306 0.07-0.15 wt.%; Cr# of chromite: 23-89) (Suhr et al., 2003; Piccardo et al., 2007;
307 Ackerman et al., 2009; Mazzucchelli et al., 2009; Oh et al., 2012; Sanfilippo et al.,
308 2014, 2017) (Fig. 4), indicating that these dunites were formed by melt-peridotite

interaction rather than have a cumulate origin. Furthermore, although the olivines from these dunites show a good correlation between Ni and Mn, the correlation between Co and Mn is poor (Fig. 6b-c). According to olivine-melt partition coefficients (e.g., Beattie et al., 1991), Co and Ni are compatible in olivine, whereas Mn is incompatible, and hence segregation of olivine from its parental magma should produce a decrease of Co and Ni with increasing Mn (Sanfilippo et al., 2014). However, Co contents in olivine from the Orhaneli and Harmancık dunites are poorly correlated with Mn contents, and therefore incompatible with olivine fractionation and likely to be induced by melt migration.

For the Orhaneli and Harmancık ophiolites, the mineralogical and geochemical characteristics of mantle-crust transition zone dunites indicate that they were formed by melt-peridotite interaction: orthopyroxene + melt 1 → olivine + melt 2. In this reaction, melt 1 (reactant) is silica-undersaturated and melt 2 (product) is relatively enriched in SiO_2 and Cr_2O_3 due to progressive melt-rock reaction (e.g., Suhr, 1999; Zhou et al., 2005). Since the majority of all dunites are of refractory chemical nature and not akin to MORB (Figs. 4, 6), we argue that the reactant (melt 1) was highly depleted.

6.2 Origin of chromitites of the Orhaneli and Harmancık ophiolites

Olivines in Orhaneli and Harmancık chromitites have somewhat higher Fo than that contained in dunites, which likely implies an additional process for the chromitites. Subsolidus Mg-Fe exchange between olivine and chromite has been

usually reported in chromitites (e.g., Xiao et al., 2016):

$$FeSiO_4 + MgCr_2O_4 = MgSiO_4 + FeCr_2O_4 \quad \text{(Eq. 1)}$$

The Mg diffuses from chromite to olivine and Fe from olivine to chromite. The compositional effect of Fe-Mg exchange on olivine depends on the elemental contents and relative modal abundances of olivine and chromite in the rocks (Xiao et al., 2016). The Fe-Mg exchange effect on olivine in the dunites is negligible because of the extremely low amount of chromite. Recent studies (e.g., Qian et al., 2010) reported that despite differences in ionic size and charge, Sc and V diffuse at approximately similar rates to Mg, Fe and other divalent cations (e.g., Co and Zn). Cobalt and Zn are more compatible in chromite than in olivine, with crystal-melt partition coefficients from 8.3 to 2.1, and 7.9 to 3.6, respectively (https://earthref.org). Vanadium compatibility decreases in the order of chromite >> pyroxene >> olivine (Witt-Eickschen and O'Neill et al., 2005). In addition, the partitioning of Sc between chromite and olivine is strongly dependent upon the major element composition of chromite (Stosch et al., 1981). Thus, as expected, Co, Zn, Sc and V concentrations of olivine in the Orhaneli profile and Harmancık chromitites are lower than those in the associated dunites (Figs. 5a-b), which points to the relative modal abundances of chromite and olivine being a factor in determining the Sc, V, Co and Zn concentrations in olivine in chromitites (Xiao et al., 2016; Zhang et al., 2017). For example, in the Orhaneli profile, chromitite sample (+50 m) contains the highest modal amount of chromite and its olivine has the lowest Co, Zn, Sc and V concentrations (Fig. 5a).

353 Mantle-derived magmas generally have ca. 500 ppm Cr concentrations, whereas
354 the chromites derived from these melts contain 30-50 wt.% Cr_2O_3 (Zhou et al., 2014;
355 Zhang et al., 2017). During the evolution of magmatic systems, the oversaturation of
356 chromite in the magma is an important factor for the formation of chromitite. Addition
357 of silica to magmas has been widely accepted as a means of triggering chromite
358 precipitation, because SiO_2 addition can decrease Cr solubility (Irvine et al., 1986).
359 The increase in silica has been usually attributed to assimilation/reaction of more
360 siliceous materials or magma mixing (e.g., Arai et al., 2004; Zhou et al., 1994, 2014;
361 Zhang et al., 2017). In this regard, chromitites in the Orhaneli and Harmancık
362 mantle-crust transition zones are exclusively associated with dunites, and hence it is
363 unlikely that the oversaturation of chromite was caused by extensive assimilation of
364 siliceous-rich crust. Instead, the oversaturation of chromite induced by magma mixing
365 becomes the most likely scenario here. Mantle-derived mafic magma A rises through
366 the upper mantle and mixes with more Si-rich and Cr-rich magma (e.g., Lissenberg
367 and Dick, 2008), upon which the newly-formed, mixed magma B would move into
368 the field of chromite crystallization (Fig. 9). Additionally, the residual melt (melt 2)
369 following melt-peridotite reaction and orthopyroxene dissolution will also be enriched
370 with Cr and SiO_2 relative to the infiltrating melt (Arai and Yurimoto, 1995).
371 Therefore, it would further facilitate the oversaturation of chromite in the mixed
372 magma (Zhou et al., 1994, 2014; Su et al., 2019), driving crystallization of abundant
373 chromite and forming chromitite layers. Due to precipitation of chromite, mixed
374 magma ‘B’ would evolve to point ‘C’, i.e., back to the chromite-olivine cotectic line.

375

376 **6.3 Origin of infiltrating melts**

377 During melt-peridotite interaction, trace elements between minerals and melts
378 can be redistributed. The trace elements of olivine in the Orhaneli and Harmancık
379 dunites do not show any zoning (Tables S1, S3), indicating that they were fully
380 equilibrated with the percolating melts. Since dunites predominantly consist of olivine
381 grains, and other silicate minerals (e.g., pyroxene) are rare or absent, the trace element
382 concentrations of olivine cannot be affected by subsolidus re-equilibration among
383 silicate minerals. Thus, the olivine trace elements can be used to trace the composition
384 of the melt in chemical equilibrium with these crystals. The lower incompatible trace
385 element concentrations (Zr, Ti and HREE) in olivines from the Orhaneli and
386 Harmancık dunites relative to those of the olivines from the lower crustal sections of
387 ophiolites (Sanfilippo et al., 2014) (Fig. 6a) indicate that our dunites are not in
388 equilibrium with a melt derived from the lower oceanic crust. In addition, compared
389 to mantle harzburgites of the Orhaneli and Harmancık ophiolites (chromite Cr#: 43-55;
390 Fo < 91.6) (Uysal et al., 2017), the mantle-crust transition zone dunites have Cr# in
391 chromite of 79-82, NiO in olivine of 0.2-0.4 wt.% and Fo of 91.6-94.0, which are far
392 more refractory. The Mn and Co abundances of olivines in both the Orhaneli and
393 Harmancık dunites are lower than those of olivine phenocrysts within MORB
394 (Sobolev et al., 2007) (Fig. 6b-c), in conjunction with the lower trace-element
395 concentrations relative to primitive mantle (McDonough and Sun, 1995), suggesting
396 that these dunites were equilibrated with melts that are more depleted than MORB

(e.g., Piccardo et al., 2004; Sanfilippo and Tribuzio, 2011).

We can use the composition of the chromitites to put further constraints on the composition of its parental melts. In contrast to the incompatible elements, diffusion of compatible elements Cr, Al and Ti out of chromite is negligible (Abily and Ceuleneer, 2013), because Al and Ti enter olivine and/or serpentine in only very low amounts (e.g., Kamenetsky et al., 2001). As a consequence, we can use these elements to calculate the composition of equilibrated melts based on chromite compositions. The TiO_2 content of chromite is a key indicator of tectonic setting of where chromitite forms (e.g., Kamenetsky et al., 2001). The Orhaneli and Harmancık chromites have very low TiO_2, and plot in the arc or boninitic fields (Fig. 10a-b), suggesting crystallization from low-Ti island arc tholeiitic melts or boninitic melts. In addition, several studies have also shown that chromite compositions in chromitites reflect the composition of their parental melt (Kamenetsky et al., 2001; Rollinson, 2008; Zhou et al., 2014; Rollinson and Adetunji, 2015; Chen et al., 2019). The following equations were proposed by Rollinson and Adetunji (2015) to more closely reflect the empirical correlations defined by Kamenetsky et al. (2001) and applies to melt with an arc affinity:

$$(Al_2O_3)_{melt} = 5.2181 \times \ln(Al_2O_3)_{Chr} - 1.0505 \quad \text{(Eq. 2)}$$

$$(TiO_2)_{melt} = 1.0963 \times (TiO_2)_{Chr}^{0.7863} \quad \text{(Eq. 3)}$$

The implementation of equations (2) and (3) demonstrates that the melts in equilibrium with chromitite have the following composition: 9.8-10.8 wt.% Al_2O_3 and 0.23-0.38 wt.% TiO_2 in Orhaneli, and 10.7-11.4 wt.% Al_2O_3 and 0.22-0.33 wt.% TiO_2

in Harmancık. The inferred parental melts of the chromitites from the two ophiolites have similar Al_2O_3 and TiO_2 contents to boninitic melts (Fig. 10c), suggesting that the Orhaneli and Harmancık chromitites possibly originated in a forearc setting during the early stage of subduction. The zigzag pattern (Fig. 5) of the olivine trace element contents in the chromitites from the Orhaneli profile and Harmancık drill hole, in conjunction with the widespread occurrence of interlayered chromitites and dunites, could be the witness of multiple magma replenishments in the mantle-crust transition zone.

6.4 Lithium isotope constraints on the origin of Orhaneli and Harmancık dunites and chromitites

Due to the highly depleted composition of dunites and chromitites, traditional chemical indicators of tectonic setting can generally not be applied. However, Li isotope systematics of olivine may provide clues about the tectonic setting of the infiltrating melts. High-temperature partial melting is thought to induce negligible Li isotope fractionation (e.g., Tomascak et al., 1999; Ionov and Seitz, 2008) and Jeffcoate et al. (2007) estimated that the δ^7Li value of magmas generated by equilibrium melting would be < 0.5‰ different from their source. In addition, most studies have shown that Li isotopes do not fractionate during fractional crystallization of silicate magmas (e.g., Tomascak et al., 1999; Teng et al., 2006). Many studies also demonstrated that diffusion is an important mechanism controlling Li abundances and isotopic distribution (e.g., Su et al., 2014; Tomascak et al., 2016). Lithium

441 concentrations and isotopes do not show core-to-rim zoning in individual olivine
442 grains in most samples of the Orhaneli and Harmancık ophiolites (Table S2), and
443 chromite contains little or no Li (e.g., Jeffcoate et al., 2007; Chen et al., 2019). Thus,
444 the Li isotopic compositions of olivine have not been affected by inter-mineral
445 diffusion. Therefore, the Li isotopic compositions of olivines in the Orhaneli and
446 Harmancık dunites record the history of melt-rock interaction.

447 Compared to typical mantle peridotites with δ^7Li values of 2-6‰ and 1.0-1.8
448 ppm Li (Seitz and Woodland, 2000; Su et al., 2014), the olivines from the Orhaneli
449 dunites show a similar range of Li concentrations (0.9-1.5 ppm), but a slightly larger
450 range of δ^7Li values (+4.0 to +11.0‰) (Table S1; Figs. 7, 8), offset to higher values.
451 As the samples are relatively homogeneous (1s 0.8-1.7‰ based on multiple olivine
452 analyses in each sample) (Fig. 7) and the olivines are unzoned, these samples likely
453 reached Li isotope equilibrium during rock-melt interaction, and therefore could
454 reflect the composition of the infiltrating melt. Average δ^7Li per sample shows a more
455 restricted range from +4.8 to +8.7‰ with 1.1-1.3 ppm Li, suggesting reaction with
456 relatively homogeneous melt batches.

457 The Orhaneli chromitites have somewhat higher δ^7Li values (average δ^7Li per
458 sample +6.0 to +10.6‰ with 1.0-1.3 ppm), but the two samples with highest δ^7Li
459 shows considerable heterogeneity (based on multiple olivine analyses in each sample)
460 of > 4-7‰ even though individual olivines are unzoned. Excluding these samples, the
461 range of Orhaneli chromitites is +6.0 to +8.2‰, an even smaller range than the
462 dunites. These Li isotopic characteristics could be attributed to infiltrating melts in a

463 subduction zone setting. Dehydration of altered oceanic crusts during subduction can
464 induce that the Li isotope fractionation generates isotopically heavy-Li fluids and
465 light-Li slab residues (e.g., Elliott et al., 2004; Penniston-Dorland et al., 2017), but the
466 Li isotopic range of arc lavas (-1 to +12‰) reflects the heterogeneity of the altered
467 oceanic plate and overlying sediments (Tomascak et al., 2002; Elliott et al., 2004).
468 Mixing of various slab components and re-equilibration with Li already present in the
469 mantle wedge results in arc lavas with δ^7Li values that only slightly extend beyond
470 that of MORB. The dominance of δ^7Li values in the Orhaneli mantle-crust transition
471 zone that extends well beyond the MORB/mantle peridotite range point to a
472 ubiquitous subducting slab component present in the infiltrating melts. The survival of
473 these signatures suggests that the source of the interacting agent was rather shallow,
474 as Li isotopic signatures will re-equilibrate with ambient mantle at short length and
475 timescales (Halama et al., 2009). This is consistent with a subduction initiation.

476 Compared to Orhaneli, olivine from the Harmancık dunites shows much larger
477 δ^7Li variations of -2.5‰ up to +20.3‰, but also larger sample heterogeneity, with
478 only one sample having a ranging of δ^7Li of < 3‰ (Figs. 7, 8). The Harmancık
479 dunites were considerably more altered than the Orhaneli dunites, but the olivine
480 grains selected for Li isotope analyses were fresh and unzoned, and hence the
481 influences of alteration (such as serpentinization) on δ^7Li values between different
482 grains are likely to be small (e.g., Lundstrom et al., 2005). The larger range of δ^7Li
483 values in the Harmancık dunite may indicate the infiltrating melts with a wider range
484 of δ^7Li values, especially given that the slab-derived fluids and melts have a broad

485 range of compositions and are highly variable from one location to another (Elliott et
486 al., 2004; Yao et al., 2018). However, the heterogeneous distribution of δ^7Li in
487 individual samples from the Harmancık dunites and the negative correlation between
488 δ^7Li values and Li concentrations is indicative of incomplete diffusive equilibration
489 between olivines and infiltrating melts (Fig. 8) (e.g., Jeffcoate et al., 2007;
490 Penniston-Dorland et al., 2017), which is consistent with the studies of olivine Li
491 isotope of dunite from Trinity ophiolite (Lundstrom et al., 2005) and Luobusa
492 ophiolite (Su et al., 2016). Many studies have demonstrated that ^{6}Li diffuses about 2-3%
493 faster than ^{7}Li through melts and minerals (e.g., Lundstrom et al., 2005; Teng et al.,
494 2006). As Li diffuses from percolating melt into olivine, the δ^7Li of olivine will
495 become lower at first, but will then increase to higher values until δ^7Li equilibrates
496 with that of the infiltrating melt, due to equilibrium partitioning (Lundstrom et al.,
497 2005). During this process, temperature and time are the fundamental parameters that
498 control the efficiency of the isotopic exchange (Tomascak et al., 2016). We, therefore,
499 estimated the equilibration temperatures of the Harmancık and Orhaneli dunites and
500 chromitites based on the Al (Coogan et al., 2014) and Mg-Fe exchange (Ballhaus et
501 al., 1991) between olivine and chromite (Table 1). The Al-in-olivine thermometry
502 results (Coogan et al., 2014) show that the temperature range for Harmancık dunites
503 (933-979°C) is similar to that of the Orhaneli suite (960-993°C), while Mg-Fe
504 exchange temperatures (Ballhaus et al., 1991) are considerably lower: 714-778°C for
505 Orhaneli dunites and 663-755°C for Harmancık dunites. This suggests no significant
506 difference in temperature between Harmancık and Orhaneli ophiolites, so this cannot

507 explain the heterogeneity of the Harmancık samples. The main another factor of
508 diffusion is time. Richter et al. (2014) found that very large lithium isotopic
509 fractionations persisted after the lithium concentration had become effectively
510 homogenized during diffusion process, suggesting that it still takes longer for the
511 isotopic composition to become uniform compared to the time it takes for diffusion to
512 homogenize the total lithium concentration. Thus, if infiltration of melts into the rocks
513 occurred shortly before obduction and exhumation, Li isotopes would not fully
514 equilibrate, and isotope heterogeneity would be preserved during relatively rapid
515 cooling. Heterogeneities in the Harmancık samples could indicate rapid cooling was
516 essential to preserve the observed isotope heterogeneities.

517 In summary, excluding two heterogeneous samples (Fig. 7), the Li isotope
518 signatures of olivine in dunites and chromitites from the Orhaneli ophiolite are likely
519 primary features inherited from their parental melts, with all olivines falling between
520 δ^7Li values of +5‰ and +9‰, which is within the range of arc lavas but isotopically
521 heavier than MORB (Fig. 7) (Chan et al., 2002; Tomascak et al., 2002), suggesting an
522 affinity with arc magmatism. The olivine Li isotopic compositions of Harmancık
523 mantle-crust transition zone chromitites are similar to those from Orhaneli, but still,
524 likely have diffusional heterogeneities due to incomplete equilibration between
525 infiltrating melt and olivine. Nevertheless, their average compositions (+6 to +11‰)
526 does suggest a melt source similar to the one that crystallized Orhaneli chromitites.

527 The estimated Al_2O_3 and TiO_2 contents of the parental magmas of chromitites in
528 the two ophiolites are similar to the signatures of boninitic melts. Given that boninitic

529 magmas have been widely found in preserved fore-arcs related to subduction
530 initiation (e.g., Reagan et al., 2017; Stern et al., 2012), this suggests that the Orhaneli
531 and Harmancık ophiolites possibly originated in a subduction initiation setting, which
532 gives additional support to studies suggesting that these settings represent an ideal
533 environment for forming ophiolites with economically viable chromitite deposits
534 (Johnson, 2012).
535
536 **7 Conclusions**
537 This study presents in-situ trace elements and Li isotopic compositions of olivine
538 in dunites and chromitites from the Orhaneli and Harmancık mantle-crust transition
539 zone. The following conclusions can be drawn:
540 1. Compared to olivine from cumulate dunites, the olivine in the Orhaneli and
541 Harmancık dunites is distinct by higher Ni, lower Mn concentrations and extreme
542 depletion of incompatible trace elements (Ti, Zr and HREE), which are consistent
543 with the formation of dunites driven by interaction of peridotite with depleted
544 melts.
545 2. The relatively uniform Li isotopic compositions (+4 to +11‰) of olivines from
546 Orhaneli dunites indicate these samples reached Li isotope equilibrium, and
547 suggest a reaction driven by relatively homogeneous melt batches with a
548 subduction component, whereas the large δ^7Li variations (-2.5 to +20.3‰) in
549 olivine from Harmancık dunites reflect incomplete diffusive equilibration during
550 the melt percolation through these dunites.

3. The formation of chromitites in the mantle-crust transition zone of the two ophiolites was likely triggered by the magma mixing. The calculated Al_2O_3 (9.8-11.4 wt.%) and TiO_2 (0.22-0.38 wt.%) contents of the parental magmas of chromitites demonstrate a boninite-like geochemical affinity, i.e., a subduction initiation setting, which is in good agreement with the Li isotopic compositions of their olivines.
4. In contrast to the dunites, the higher Fo contents of olivine in the chromitites could be caused by the Mg-Fe exchange between olivine and chromite. The lower Sc, V, Co and Zn concentrations of olivine in the chromitites are controlled by the modal abundances of chromite.

Acknowledgements

This paper benefited from constructive and detailed comments of two anonymous reviewers, and efficient editorial handling by Xian-Hua Li. This study was supported by the National Natural Science Foundation of China (Grants 91755205 and 41772055), and by a Visiting Student grant to Chen Chen from the United Kingdom National Environment Research Council 'Deep Volatiles' program (Grant NE/M000427/1). We thank Wei Lin, Yang Chu and Jie-Jun Jing for the assistance in the field trips in the Kızıldağ.

References

Abily, B., Ceuleneer, G., 2013. The dunitic mantle-crust transition zone in the Oman ophiolite: residue of melt-rock interaction, cumulates from high-MgO melts, or

573 both? Geology 41, 67-70.
574 Ackerman, L., Jelínek, E., Medaris Jr., G., Ježek, J., Siebel,W., Strnad, L., 2009.
575 Geochemistry of Fe-rich peridotites and associated pyroxenites from Horní Bory,
576 Bohemian Massif: insights into subduction-related melt-rock reactions. Chemical
577 Geology 259, 152-167.
578 Anders, E., Ebihara, M., 1982. Solar system abundances of the elements. Geochimica
579 et Cosmochimica Acta 46, 2363-2380.
580 Arai, S., Ishimaru, S., Mizukami, T., 2012. Methane and propane micro-inclusions in
581 olivine in titanoclinohumite-bearing dunites from the Sanbagawa high-P
582 metamorphic belt, Japan: hydrocarbon activity in a subduction zone and Timobility.
583 Earth and Planetary Science Letters 354, 1-11.
584 Arai, S., Yurimoto, H., 1995. Possible sub-arc origin of podiform chromitites. Island
585 Arc 4, 104-111.
586 Arai, S., Uesugi, J., Ahmed, A.H., 2004. Upper crustal podiform chromitite from the
587 northern Oman ophiolite as the stratigraphically shallowest chromitite in ophiolite
588 and its implication for Cr concentration. Contributions to Mineralogy and Petrology
589 147, 145-154.
590 Ballhaus, C., 1998. Origin of podiform chromite deposits by magma mingling. Earth
591 and Planetary Science Letters 156, 185-193.
592 Ballhaus, C., Berry, R.F., Green, D.H., 1991. High pressure experimental calibration
593 of the olivine-orthopyroxene-spinel oxygen geobarometer: implications for the
594 oxidation state of the upper mantle. Contributions to Mineralogy and Petrology 107,

595 27-40.
596 Beattie P., Ford, C., Russell, D., 1991. Partition coefficients for olivine-melt and
597 orthopyroxene-melt systems. Contributions to Mineralogy and Petrology 109,
598 212-224.
599 Chan, L.H., Alt, J.C., Teagle, D.A.H., 2002. Lithium and lithium isotope profiles
600 through the upper oceanic crust: a study of seawater-basalt exchange at ODP Sites
601 504B and 896A. Earth and Planetary Science Letters 201, 187-201.
602 Chen, C., Su, B.X., Xiao, Y., Pang, K.N., Robinson, P.T., Uysal, İ., Lin, W., Qin, K.Z.,
603 Avcı, E., Kapsiotis, A., 2019. Intermediate chromitite in Kızıldağ ophiolite (SE
604 Turkey) formed during subduction initiation in Neo-Tethys. Ore Geology Reviews
605 104, 88-100.
606 Chen, C., Su, B.X., Xiao, Y., Lin, W., Chu, Y., Liu, X., Bai, Y., 2018. Geological
607 records of subduction initiation of Neo-Tethyan ocean: ophiolites and metamorphic
608 soles in southern Turkey. Acta Petrologica Sinica 34, 3302-3314 (in Chinese with
609 English abstract).
610 Coogan, L.A., Saunders, A.D., Wilson, R.N., 2014. Aluminum-in-olivine
611 thermometry of primitive basalts: evidence of an anomalously hot mantle source
612 for large igneous provinces. Chemical Geology 368, 1-10.
613 De Hoog, J.C.M., Gall, L., Cornell, D.H., 2010. Trace-element geochemistry of
614 mantle olivine and application to mantle petrogenesis and geothermobarometry.
615 Chemical Geology 270, 196-215.
616 Derbyshire, E.J., O'Driscoll, B., Lenaz, D., Gertisser, R., Kronz, A., 2013.

617 Compositionally heterogeneous podiform chromitite in the Shetland ophiolite
618 complex (Scotland): Implications for chromitite petrogenesis and late-stage
619 alteration in the upper mantle portion of a supra-subduction zone ophiolite. Lithos
620 162, 279-300.
621 Dilek, Y., Thy, P., 2006. Age and petrogenesis of plagiogranite intrusions in the
622 Ankara mélange, Central Turkey. Island Arc 15, 44-57.
623 Elliott, T., Jefcoate,A., Bouman, C., 2004. The terrestrial Li isotope cycles:
624 light-weight constraints on mantle convection. Earth and Planetary Science Letters
625 220, 231-245.
626 Foley, S.F., Prelevic, D., Rehfeldt, T., Jacob, D.E., 2013. Minor and trace elements in
627 olivines as probes into early igneous and mantle melting processes. Earth and
628 Planetary Science Letters 363, 181-191.
629 Foley, S.F., Jacob, D.E., O'Neill, H.S.C., 2011. Trace element variations in olivine
630 phenocrysts from Ugandan potassic rocks as clues to the chemical characteristics of
631 parental magmas. Contributions to Mineralogy and Petrology 162, 1-20.
632 Halama, R., Savov, I.P., Rudnick, R.L., McDonough, W.F., 2009. Insights into Li and
633 Li isotope cycling and sub-arc metasomatism from veined mantle xenoliths,
634 Kamcharka. Contributions to Mineralogy and Patrology 158, 197-222.
635 Ionov, D.A., Seitz, H.M., 2008. Lithium abundances and isotopic compositions in
636 mantle xenoliths from subduction and intra-plate settings: mantle sources vs.
637 eruption histories. Earth and Planetary Science Letters 266, 316-331.
638 Irvine, T.N., Sharpe, M.R., Gallagher, M.L., 1986. Magma mixing and the origin of

639 stratiform oxide ore zones in the Bushveld and Stillwater complexes. Metallogeny
640 of Basic and Ultrabasic Rocks, 183-198.
641 Jeffcoate, A.B., Elliott, T., Kasemann, S.A., Ionov, D., Cooper, K., Brooker, R., 2007.
642 Li isotope fractionation in peridotites and mafic melts. Geochimica et
643 Cosmochimica Acta 71, 202-218.
644 Johnson, C., 2012. Podiform chromite at Voskhod, Kazakhstan. Unpublished PhD
645 Thesis. Cardiff University. http://orca.cf.ac.uk/40714/
646 Kamenetsky, V.S., Crawford, A.J., Meffre, S., 2001. Factors controlling chemistry of
647 magmatic spinel: an empirical study of associated olivine, Cr-spinel and melt
648 inclusions from primitive rocks. Journal of Petrology 42, 655-671.
649 Lissenberg, C.J., Dick, H.J.B., 2008. Melt-rock reaction in the lower oceanic crust and
650 its implications for the genesis of mid-ocean ridge basalt. Earth and Planetary
651 Science Letters 271, 311-325
652 Lundstrom, C.C., Chaussidon, M., Hsui, A.T., Kelemen, P., Zimmerman, M., 2005.
653 Observations of Li isotopic variations in the Trinity Ophiolite: evidence for isotopic
654 fractionation by diffusion during mantle melting. Geochimica et Cosmochimica
655 Acta 69, 735-751.
656 Mazzucchelli, M., Rivalenti, G., Brunelli, D., Zanetti, A., Boari, E., 2009. Formation
657 of highly refractory dunite by focused percolation of pyroxenite-derived melt in the
658 Balmuccia Peridotite Massif (Italy). Journal of Petrology 50, 1205-1233.
659 McDonough, W.F., Sun, S.S., 1995. The composition of the Earth. Chemical Geology
660 20, 223-253.

661 Oh, C.W., Seo, J., Choi, S.G., Rajesh, V.J., Lee, J.H., 2012. U-Pb SHRIMP zircon
662 geochronology, petrogenesis, and tectonic setting of the Neoproterozoic Baekdong
663 ultramafic rocks in the Hongseong Collision Belt, South Korea. Lithos 131,
664 100-112.
665 Paktunc, A.D., 1990. Origin of podiform chromite deposits by multistage melting,
666 melt segregation and magma mixing in the upper mantle. Ore Geology Reviews 5,
667 211-222.
668 Pearce, J.A., Barker, P.F., Edward, S.J., Parkinson, I.J., Leat, P.T., 2000. Geochemistry
669 and tectonic significance of peridotites from the south Sandwich arc-basin system,
670 south Atlantic. Contributions to Mineralogy and Petrology 139, 36-53.
671 Peighambari, S., Uysal, İ., Stosch, H.G., Ahmadipour, H., Heidarian, H., 2016.
672 Genesis and tectonic settings of ophiolitic chromitites from the Dehsheikh
673 ultramafic complex (Kerman, southeastern Iran): inferences from platinum-group
674 elements and chromite compositions. Ore Geology Reviews 74, 39-51.
675 Penniston-Dorland, S., Liu, X.M., Rudnick, R.L., 2017. Lithium isotope geochemistry.
676 Reviews in Mineralogy and Geochemistry 82, 165-217.
677 Piccardo, G.B., Zanetti, A., Muntener, O., 2007. Melt/peridotite interaction in the
678 Southern Lanzo peridotite: field, textural and geochemical evidence. Lithos 94,
679 181-209.
680 Piccardo, G.B., Müntener, O., Zanetti, A., Pettke, T., 2004. Ophiolitic peridotites of
681 the Alpine-Apennine system: mantle processes and geodynamic
682 relevance. International Geology Review 46, 1119-1159.

683 Qian, Q., O'Nell, H.S.C., Hermann, J., 2010. Comparative diffusion coefficients of
684 major and trace elements in olivine ~950°C from a xenocryst included in dioritic
685 magma. Geology 4, 331-334.
686 Rampone, E., Borghini, G., Godard, M., Ildefonse, G., Cridpini, L., Fumagalli, P.,
687 2016. Melt/rock reaction at oceanic peridotite/gabbro transition as revealed by trace
688 element chemistry of olivine. Geochemica et Cosmochimica Acta 190, 309-331.
689 Reagan, M.K., Pearce, J.A., Petronotis, K., Almeev, R.R., Avery, A.J., Carvallo, C.,
690 Chapman, T., Christeson, G.L., Ferré, E.C., Godard, M., Heaton, D.E., Kirchenbaur,
691 M., Kurz, W., Kutterolf, S., Li, H.Y., Li, Y.B., Michibayashi, K., Morgan, S.,
692 Nelson, W.R., Prytulak, J., Python, M., Robertson, A.H.F., Ryan, J.G., Sager, W.W.,
693 Sakuyama, T., Shervais, J.W., Shimizu, K, Whattam, S.A., 2017. Subduction
694 initiation and ophiolite crust: new insights from IODP drilling. International
695 Geology Review 59, 1439-1450.
696 Richter, F., Watson, B., Chaussidon, M., Mendybaev, R., Ruscitto, D., 2014. Lithium
697 isotope fractionation by diffusion in minerals. Part I: pyroxenes. Geochimica et
698 Cosmochimica Acta 126, 352-370.
699 Rollinson, H., Mameri, L., Barry, T., 2018. Polymineralic inclusion in mantle
700 chromitites from the Oman ophiolite indicate a highly magnesian parental melt.
701 Lithos 310, 381-391.
702 Rollinson, H., Adetunji, J., 2015. The geochemistry and oxidation state of podiform
703 chromitites from the mantle section of the Oman ophiolite: a review. Gondwana
704 Research 27, 543-554.

Rollinson, H., 2008. The geochemistry ofmantle chromitites from the northern part of the Oman ophiolite: inferred parental melt composition. Contributions to Mineralogy and Petrology 156, 273-288.

Rospabé, M., Benoit, M., Ceuleneer, G., Hodel, F., Kaczmarek, M.A., 2018. Extreme geochemical variability through the dunitic transition zone of the Oman ophiolite: implications for melt/fluid reactions at Moho level beneath oceanic spreading centres. Geochimica Cosmochimica Acta 234, 1-23.

Rudnick, R.L., Ionov, D.A., 2007. Lithium elemental and isotopic disequilibrium in minerals from peridotite xenoliths from far-east Russia: product of recent melt/ fluid-rock reaction. Earth and Planetary Science Letters 256, 278-293.

Sanfilippo, A., Tribuzio, R., Ottolini, L., Hamada, M., 2017. Water, lithium and trace element compositions of olivine from Lanzo South replacive mantle dunite (western Alps): new constraints into melt migration processes at cold thermal regimes. Geochimica et Cosmochimica Acta 214, 51-72.

Sanfilippo, A., Tribuzio, R., 2011. Melt transport and deformation history in a non-volcanic ophiolitic section northern Apennine, Italy: implications for crustal accretion at slow spreading settings. Geochemistry, Geophysics, Geosystems 12, Q0AG04.

Santos, J.F., Schärer, U., Ibarguchi, J.I.G., Girardeau, J., 2002. Genesis of pyroxenite-rich peridotite at Cabo Ortegal (NW Spain): geochemical and Pb-Sr-Nd isotope data. Journal of Petrology 43, 17-43.

726 Sarıfakıoğlu, E., Dilek, Y., Sevin, M., 2017. New synthesis of the
727 Izmir-Ankara-Erzincan suture zone and the Ankara mélange in northern Anatolia
728 based on new geochemical and geochronological constraints. Geological Society of
729 America Special paper 525, 1-62.
730 Sarıfakıoğlu, E., Ozen, H., Winchester, J.A., 2009. Whole rock and mineral chemistry
731 of ultramafic-mafic cumulates from the Orhaneli (Bursa) ophiolite, NW Anatolia.
732 Turkish Journal of Earth Sciences 18, 55-83.
733 Seitz, H.M., Woodland, A.B., 2000. The distribution of lithium in peridotitic and
734 pyroxenitic mantle lithologies - an indicator of magmatic and metasomatic
735 processes. Chemical Geology 166, 47-64.
736 Seo, J., Oh, C.W., Choi, S.G., Rajesh, V.J., 2013. Two ultramafic rock types in the
737 Hongseong area, south Korea: tectonic significance for northeast Asia. Lithos 176,
738 30-39.
739 Sobolev, A.V., Hofmann, A.W., Kuzmin, D.V., Yaxley, G.M., Arndt, N.T., Chung, S.L.,
740 Danyushevsky, L.V., Elliott, T., Frey, F.A., Garcia, M.O., Gurenko, A.A.,
741 Kamenetsky, V.S., Kerr, A.C., Krivolutskaya, N.A., Matvienkov, V.V., Nikogosian,
742 I.K., Rocholl, A., Sigurdsson, I.A., Sushchevskaya, N.M., Teklay, M., 2007. The
743 amount of recycled crust in sources of mantle-derived melts. Science 316, 412-417.
744 Song, S.G., Su, L., Niu, Y.L., Zhang, L.F., Zhang, G.B., 2007. Petrological and
745 geochemical constraints on the origin of garnet peridotite in the North Qaidam
746 ultrahigh-pressure metamorphic belt, northwestern China. Lithos 96, 243-265.

747 Stern, R.J., Reagan, M., Ishizuka, O., Ohara, Y., Whattam, S., 2012. To understand
748 subduction initiation, study forearc crust: to understand forearc crust, study
749 ophiolites. Lithosphere 4, 469-483.
750 Stosch, H.G., 1981. Sc, Cr, Co and Ni partitioning between minerals from spinel
751 peridotite xenoliths. Contributions to Mineralogy and Petrology 78, 166-174.
752 Suhr, G., Hellebrand, E., Snow, J.E., Seck, H.A., Hofmann, A.W., 2003. Significance
753 of large, refractory duninte bodies in the upper mantle of the Bay of Island
754 ophiolite. Geochemistry, Geophysics, Geosystems 4.
755 Suhr, G., 1999. Significance of upper mantle hosted dunite bodies for melt migration
756 and extraction under oceanic spreading centres: inferences from reactive transport
757 modelling. Journal of Petrology 40, 575-599.
758 Su, B.X., Zhou, M.F., Jing, J.J., Robinson, P., Chen, C., Xiao, Y., Liu, X., Shi, R.D.,
759 Lenaz, D., Hu, Y., 2019. Distinctive melt activity and chromite mineralization in
760 Luobusa and Purang ophiolites, southern Tibet: constraints from trace element
761 compositions of chromite and olivine. Science Bulletin 64, 108-121.
762 Su, B.X., Zhou, M.F., Robinson, P.T., 2016. Extremely large fractionation of Li
763 isotopes in a chromitite-bearing mantle sequence. Scientific Reports 6, 22370.
764 Su, B.X., Gu, X.Y., Deloule, E., Zhang, H.F., Li, Q.L., Li, X.H., Vigier, N., Tang,
765 Y.J., Tang, G.Q., Liu, Y., Brewer, A., Mao, Q., Ma, Y.G., 2015. Potential
766 orthopyroxene, clinopyroxene and olivine reference materials for in-situ lithium
767 isotope determination. Geostandards and Geoanalytical Research 39, 357-369.

768 Su, B.X., Zhang, H.F., Deloule, E., Vigier, N., Hu, Y., Tang, Y.J., Xiao, Y., Sakyi,
769 P.A., 2014. Distinguish silicate and carbonatite mantle metasomatism by using
770 lithium and its isotopes. Chemical Geology 381, 67-77.
771 Tankut, A., 1980. The Orhaneli massif, Turkey ophiolites. Geological Survey
772 Department Nicosia, 702-713.
773 Teng, F.Z., McDonough, W.F., Rudnick, R.L., Walker, R.J., Sirbescu, M.L.C., 2006.
774 Lithium isotopic systematics of granites and pegmatites from the Black Hills, South
775 Dakota. American Mineralogist 91, 1488-1498.
776 Tomascak, P.B., Magna, T., Dohmen, R., 2016. Advances in Lithium Isotope
777 Geochemistry. Springer International Publishing Switzerland, 1-195.
778 Tomascak, P.B., Tera, F., Helz, R.T., Walker, R.J., 1999. The absence of lithium
779 isotope fractionation during basalt differentiation: new measurements by
780 multicollector sector ICP-MS. Geochimica et Cosmochimica Acta 63, 907-910.
781 Tomascak, P.B., Langmuir, C.H., le Roux, P.J., Shirey, S.B., 2008. Lithium isotopes
782 in global mid-ocean ridge basalts. Geochimica et Cosmochimica Acta 72,
783 1626-1637.
784 Tomascak, P.B., Widom, E., Benton, L.D., Goldstein, S.L., Ryan, J.G., 2002. The
785 control of lithium budgets in island arcs. Earth and Planetary Science Letters 196,
786 227-238.
787 Uysal, İ., Dokuz, A., Kapsiotis, A., Saka, S., Karslı, O., Kaliwoda, M., Müller, D.,
788 2017. Petrogenesis of ultramafic rocks from the eastern Orhaneli ophiolite, NW
789 Turkey: hints on the initiation and evolution of melt-peridotite interaction processes

790 within a heterogeneously depleted mantle section. Journal of Asian Earth
791 Sciences 148, 51-64.
792 Uysal, İ., Akmaz, R.M., Kapsiotis, A., Demir, Y., Saka, S., Avcı, E., Muller, D., 2015.
793 Genesis and geodynamic significance of chromitites from the Orhaneli and
794 Harmancik ophiolites (Bursa, NW Turkey) as evidenced by mineralogical and
795 compositional data. Ore Geology Reviews 65, 26-41.
796 Uysal, İ., Şen, A.D., Ersoy, E.Y., Dilek, Y., Saka, S., Zaccarini, F., Escayola, M.,
797 Karslı, O., 2014. Geochemical make-up of oceanic peridotites from NW Turkey
798 and the multi-stage melting history of the Tethyan upper mantle. Mineralogy and
799 Petrology 108, 49-69.
800 Vlastelic, I., Koga, K., Chauvel, C., Jacques, G., Telouk, P., 2009. Survival of lithium
801 isotopic heterogeneities in the mantle supported by HIMU-lavas from Rurutu Island,
802 Austral Chain. Earth and Planetary Science Letters 286, 456-466.
803 Witt-Eickschen, G., O'Neill, H.S.C., 2005. The effect of temperature on the
804 equilibrium distribution of trace elements between clinopyroxene, orthopyroxene,
805 olivine and spinel in upper mantle peridotite. Chemical Geology 221, 65-101.
806 Xiao, Y., Teng, F.Z., Su, B.X., Hu, Y., Zhou, M.F., Zhu, B., Shi, R.D., Huang, Q.S.,
807 Gong, X.H. He, Y.S., 2016. Iron and magnesium isotopic constraints on the origin
808 of chemical heterogeneity in podiform chromitite from the Luobusa ophiolite, Tibet.
809 Geochemistry, Geophysics, Geosystems 17, 940- 953.
810 Yao, Z.S., Qin, K.Z., Mungall, J.E., 2018. Tectonic controls on Ni and Cu contents of
811 primary mantle-derived magmas for the formation of magmatic sulfide deposits.

812 American Mineralogist 103, 1545-1567.
813 Zhang, P.F., Zhou, M.F., Su, B.X., Uysal, İ., Robinson, P.T., Avcı, E., He, Y.S., 2017.
814 Iron isotopic fractionation and origin of chromitites in the paleo-Moho transition
815 zone of the Kop ophiolite, NE Turkey. Lithos 268, 65-75.
816 Zhou, M.F., Robinson, P.T., Su, B.X., Gao, J.F., Li, J.W., Yang, J.S., Malpas, J., 2014.
817 Compositions of chromite, associated minerals, and parental magmas of podiform
818 chromite deposits, the role of slab contamination of asthenospheric melts in
819 suprasubduction zone environments. Gondwana Research 26, 262-283.
820 Zhou, M.F., Robinson, P.T., Malpas, J., Edwards, S., Qi, L., 2005. REE and PGE
821 geochemical constraints on the formation of dunites in the Luobusa ophiolite,
822 southern Tibet. Journal of Petrology 46, 615-639.
823 Zhou, M.F., Robinson, P.T., Bai, W., 1994. Formation of podiform chromitites by
824 melt/rock interaction in the upper mantle. Mineralium Deposita 29, 98-101.
825

826 **Figure Captions:**

827 Fig. 1 (a) Map showing distribution of the continental blocks, major sutures and
828 related ophiolites in the Eastern Mediterranean region (modified after Chen et al.,
829 2018). (b) Simplified geological map of the Orhaneli and Harmancık ophiolites (after
830 Uysal et al., 2015). Red stars in (b) are the sampling locations. IASZ: Izmir-Ankara
831 Suture Zone; ITSZ: Inner-Tauride Suture Zone; BZSZ: Bitlis-Zagros Suture Zone.

832

833 Fig. 2 Photographs of field sites with numbered sampling locations and hand
834 specimens of dunites and chromitites from the Orhaneli mantle-crust transition zone.

835 (a) Banded chromitites that occur by the rhythmic layering of chromitite and dunite.
836 (b) Banded chromitite. (c) Disseminated chromitite.
837
838 Fig. 3 Back scattered electron images of thin sections of dunites and chromitites from
839 the Orhaneli (a)-(c) (sample Ol-1, 2-2 and 4-2) and Harmancık (d) (sample 71.5 m)
840 ophiolites.
841
842 Fig. 4 Plots of (a) MnO vs. Fo of olivine, (b) NiO vs. Fo of olivine, (c) Cr# of
843 chromite vs. Fo, and (d) Cr# vs. TiO_2 of chromite in dunites from the Orhaneli and
844 Harmancık ophiolites. The gray and pink fields represent literature olivine/chromite
845 composition ranges of cumulate dunites and dunites formed by peridotite-melt
846 interaction, respectively. The cumulate dunite field is defined using data from Santos
847 et al. (2002), Song et al. (2007), Arai et al. (2012) and Seo et al. (2013). The replacive
848 dunite field is defined using data from Suhr et al. (2003), Piccardo et al. (2007),
849 Ackerman et al. (2009), Mazzuchelli et al. (2009), Oh et al. (2012), Sanfilippo et al.
850 (2014, 2017).
851
852 Fig. 5 Elemental (Fo, Ni, Mn, Li, Co, Zn, Sc and V) and isotopic (δ^7Li) variations of
853 olivine compositions in the Orhaneli profile (a) and Harmancık drill hole (b). Olivine
854 grains from dunites are shown as blue circles, whereas pink circles are olivine grains
855 from chromitites. Scanned photographs of dunites and chromitites are shown to
856 clearly describe the effect of chromite proportion on olivine trace element

857 compositions.

858

859 Fig. 6 (a) Primitive mantle-normalized pattern of olivine in the dunites from Orhaneli
860 and Harmancık ophiolites. Plots of (b) Ni (ppm) vs. Mn (ppm), (c) Co (ppm) vs. Mn
861 (ppm) of olivine in the dunites from the two ophiolites. Primitive mantle values are
862 from Anders and Ebihara (1982). Compositions of lower crust data in (a) are from
863 Sanfilippo et al. (2014, 2017) and Rampone et al. (2016). The compositions of olivine
864 phenocrysts in MORB are from Sobolev et al. (2007).

865

866 Fig. 7 Li isotopic compositions of olivines in dunite and chromititesfrom the Orhaneli
867 and Harmancık ophiolites. The δ^7Li range of MORB is from Tomascak et al. (2008),
868 and the δ^7Li range of arc lava is from Tomascak et al. (2002) and Chan et al. (2002).

869

870 Fig. 8 Diagram of δ^7Li vs. Li of olivine in the Orhaneli and Harmancık dunites. The
871 arrow is the trend of Li diffusion during melt-rock interaction (after Lundstrom et al.
872 (2005)).

873

874 Fig. 9 A petrologic model for chromitite formation in the Orhaneli and Harmancık
875 ophiolites in the simplified system olivine (Ol) - quartz (Q) - chromite (Chr). The
876 trends in the phase diagrams are after Zhou et al. (1994) and Zhang et al. (2017).

877

878 Fig. 10 (a) TiO_2 vs. Al_2O_3 (after Kamenetsky et al., 2001 and Derbyshire et al., 2013),

(b) Cr# vs. TiO_2 (after Pearce et al., 2000) of chromite in the chromitites and (c) TiO_2 vs. Al_2O_3 (after Peighambari et al., 2016) of parental melts for the Orhaneli and Harmancık chromitites. FMM: fertile MORB mantle. The subscripts b and I represent boninite and island arc tholeiite, respectively. BON: boninite; IAT: island arc tholeiite; MORB: mid-ocean ridge basalt. Data of grey hexagons, triangles and circles representing lherzolite, harzburgite and dunite, respectively, are from Uysal et al. (2014).

*Revised Manuscript with changes Marked
Click here to download Revised Manuscript with changes Marked: Li-20-8-28.docx

Formation processes of dunites and chromitites in Orhaneli and Harmancık ophiolites (NW Turkey): evidence from in-situ Li isotopes and trace elements in olivine

Chen Chen[1,2,3*], Jan C.M. De Hoog[4*], Ben-Xun Su[1,3,5], Jing Wang[1,3,5], İbrahim Uysal[6], Yan Xiao[3,7]

[1] Key Laboratory of Mineral Resources, Institute of Geology and Geophysics, Chinese Academy of Sciences, Beijing 100029, China

[2] Key Laboratory of Mineralogy and Metallogeny, Guangzhou Institute of Geochemistry, Chinese Academy of Sciences, Guangzhou 510460, China

[3] Innovation Academy for Earth Science, Chinese Academy of Sciences, Beijing 100029, China

[4] Grant Institute, School of GeoSciences, The University of Edinburgh, Edinburgh, EH9 3FE, United Kingdom

[5] University of Chinese Academy of Science, Beijing, 100049, China

[6] Department of Geological Engineering, Karadeniz Technical University, 61080 Trabzon, Turkey

[7] State Key Laboratory of Lithospheric Evolution, Institute of Geology and Geophysics, Chinese Academy of Science, Beijing 100029, China

[*]Corresponding authors: chenchen2@gig.ac.cn (Chen Chen)

ceesjan.dehoog@ed.ac.uk (Jan C.M. De Hoog)

Abstract

Trace elements and Li isotopic compositions of olivine from the mantle-crust transition zone of the Bursa ophiolites (including Orhaneli ophiolite and Harmancık ophiolite) in NW Turkey were measured to constrain the genesis of these dunites and chromitites. A cumulate origin for dunite can be ruled out due to the depletion of incompatible trace elements (Zr, Ti, and heavy rare earth elements) in olivine, instead the chemical signatures point to a replacive origin via melt-rock interaction. The olivine grains in the dunites have lower MnO (0.06-0.15 wt.%), Co (106-137 ppm), and higher NiO (0.23-0.44 wt.%) concentrations than olivine phenocrysts in MORB, suggesting these transition-zone dunites have equilibrated with extremely depleted melts. Additionally, the relatively small δ^7Li variations of olivine (average δ^7Li +4.8 to +8.7‰) of the Orhaneli suite indicate the Li isotopic compositions of melts percolating through these dunites are relatively homogeneous. However, the large δ^7Li variations of olivine (-2.5 to 20.3‰) in Harmancık dunites can be explained by incomplete diffusive equilibration with melts percolating through these dunites, suggesting infiltration happened not long before obduction of the ophiolite. Olivine in chromitites has higher Fo (92.6-94.7) than coexisting dunites, likely induced by subsolidus Mg-Fe exchange between olivine and chromite. The higher chromite contents of the chromitites can also explain the lower concentrations of Sc, V, Co and Zn in coexisting olivine grains. Mixing of depleted mantle-derived melts and boninitic magmas is suggested to induce a compositional shift from the olivine-chromite cotectic line to the liquidus field of chromite, causing the precipitation of chromite

and formation of chromitite layers in the dunites. The heavy Li isotopic compositions (+6 to +11‰) of olivine in chromitites compared to MORB, together with the estimated compositions of parental magmas (Al_2O_3: 9.8-11.4 wt.%; TiO_2: 0.22-0.38 wt.%) for the chromitites, indicate an arc-like geochemical affinity, hence a subduction-related setting in which these mantle-crust transition zones formed.

Key words: olivine; trace element; Li isotopes; ophiolite; chromitite; mantle-crust transition zone

1. Introduction

The mantle-crust transition zone is well documented in many ophiolites, and marks the petrological transition from mantle peridotites to lower crustal cumulates (e.g., Zhang et al., 2017; Rollinson, et al., 2018; Rospabé et al., 2018). Ophiolitic mantle-crust transition zones typically consist of dunite-dominated ultramafic rocks and stratiform-like chromitites, and can reach a thickness of several kilometers (Paktunc, 1990). These dunites are made of mostly olivine with minor chromite and their thickness ranges from a few meters to a few hundred meters (e.g., Zhang et al., 2017). Although the transition zone chromitites are distinguished by their layered morphology from the mantle podiform chromitites which occur as irregular lenses and pods, their compositions are similar in many cases (e.g., Arai et al., 2004; Rollinson, 2008). Despite many years of investigation, the genesis of the dunites and chromitites in the ophiolitic mantle-crust transition zone is still debated, and different models have been proposed, such as magmatic cumulates stagnating at the base of the crust

(e.g., Abily and Ceuleneer, 2013), crustal assimilation (Arai et al., 2004), reactions between melts and mantle harzburgites (e.g., Abily and Ceuleneer, 2013), and mixing of mantle-derived melts with differentiated magmas (e.g., Ballhaus, 1998). In addition, the nature of the mixed or infiltrated melts and their influences on the mantle-crust transition zone are not yet well known, limiting our understanding of the evolution of ophiolites. A close link between subduction initiation and chromitite/ophiolite genesis has been documented (e.g., Reagan et al., 2017; Zhang et al., 2017) in several studies of the extensive ophiolites in Turkey (e.g., Uysal et al., 2017; Chen et al., 2019). Therefore, careful study of the formation processes of the chromitite and their tectonic setting could shine further light on the relationship between subduction initiation and ophiolite emplacement.

Olivine is a ubiquitous mineral in both the ultramafic and mafic igneous rocks, and in most cases, it is the first silicate phase to crystallize from ultramafic-mafic melts (Foley et al., 2013). Olivine thus controls early magmatic differentiation processes, but its Fo content can provide little information about its origin and evolution (De Hoog et al., 2010; Foley et al., 2013), which forces us to focus on its trace element geochemistry. Consequently, it has become increasingly important to improve our knowledge of the trace element composition of olivine, and to test the use of its geochemical signature as a tracer of early igneous and mantle melting processes (Foley et al., 2013; Rampone et al., 2016). Several studies have shown that olivines in peridotites from different tectonic environments and/or various origins exhibit distinct geochemical characteristics and define systematic elemental

correlations for a series of trace elements (Ni, Mn, Zn, Co, Zr and heavy rare earth elements (HREE)), recording different magmatic processes (Sobolev et al., 2007; De Hoog et al., 2010; Foley et al., 2013; Rampone et al., 2016). Recent work on the Purang and Luobusa ophiolites (Su et al., 2019) advocates that the incompatible trace elements of olivine are more sensitive to melting processes, whereas the concentrations of compatible trace elements are mostly constrained by their source composition.

Lithium and its isotopes (^{6}Li and ^{7}Li) are increasingly used to trace multiple high-temperature processes due to their moderate incompatibility, strong fluid mobility, and large mass difference (17%) between its two isotopes (e.g., Tomascak et al., 2016). Olivine is the dominant Li reservoir in the upper mantle (Seitz and Woodland, 2000; De Hoog et al., 2010), and olivine-melt partition coefficients of Li are virtually independent of pressure, temperature and olivine composition (Seitz and Woodland, 2000; Qian et al., 2010). The equilibrium fractionation of Li isotopes is likely to be negligible at high temperatures (Vlastelic et al., 2009). However, many natural peridotites display heterogeneous δ^{7}Li compositions, which has been attributed to Li diffusion or interaction between percolating melts and peridotites (e.g., Lundstrom et al., 2005; Rudnick and Ionov, 2007; Su et al., 2014). Thus, olivine Li isotopic systematics can be used to trace magmatic processes of mantle-crust transition zone dunites and chromitites.

In the Bursa ophiolites (Orhaneli and Harmancık ophiolites) in northwestern Turkey, mantle-crust transition zones typically contain interlayered dunites and

111 chromitites (Uysal et al., 2015), the successions of which can reach up a few
112 kilometers thick. In this paper, we provide in-situ trace element and Li isotope
113 analyses of olivine in the chromitites and dunites from the mantle-crust transition
114 zones of Orhaneli and Harmancık ophiolites. These datasets, together with
115 petrological investigations and mineral major oxide compositions, are used to
116 constrain the magmatic processes involved in the formation of dunites and chromitites
117 in ophiolitic mantle-crust transition zones.
118
119 **2. Geological Setting**
120 Tethyan ophiolites in Anatolia occur in several E-W trending belts, which are
121 separated by a series of Gondwana-derived continental fragments (e.g., Uysal et al.,
122 2014) (Fig. 1a). The Izmir-Ankara Suture Zone (IASZ) in northern Turkey occurs
123 between the Sakarya Zone (continent) to the north and the Anatolide-Tauride
124 continental block to the south (Fig. 1a), and has relatively intact ophiolite blocks,
125 which are locally extensive and well preserved (Dilek and Thy, 2006). The Orhaneli
126 and the Harmancık ophiolites, situated in the western part of the IASZ, are considered
127 as remnants of the Izmir-Ankara-Erzincan ocean, a local term for the northern branch
128 of the Neotethys ocean (Sarıfakıoğlu et al., 2009). The Orhaneli ophiolite was
129 tectonically emplaced onto northwestern Anatolia along the IASZ (Fig. 1a). The
130 Harmancık ophiolite is located ca. 30 km south of the Orhaneli ophiolite (Fig. 1b)
131 (Sarıfakıoğlu et al., 2009). These two ophiolites were thrusted southwards over the
132 metamorphic basement rocks of the Tavşanlı zone in the Anatolide-Tauride platform

133 (Sarıfakıoğlu et al., 2017).

134 The Orhaneli ophiolite is approximately 50 km long, 15 km wide and 1500 m
135 thick (Fig. 1b; Sarifakioglu et al., 2009), and mainly consists of mantle-crust
136 transition zone comprising mostly basal ultramafic cumulates. The transition zone is
137 dominated by chromitite interlayered dunites, followed by wehrlites, lherzolites,
138 harzburgites and pyroxenites and to a lesser extent mafic cumulates such as gabbros
139 and gabbronorites (e.g., Sarıfakıoğlu et al., 2009; Uysal et al., 2015). The chromitites
140 interlayer with dunite in the two ophiolites and have typically semi-massive and
141 banded (stratiform, cumulate) structures (Fig. 2). The mantle-crust transition zone of
142 the Harmancık ophiolite, which reachs up to 1000 m thickness, has similar rock
143 assemblages to those of the Orhaneli ophiolite (Tankut, 1980). The Harmancık
144 ophiolite contains additional podiform chromitites in its mantle section (Sarıfakıoğlu
145 et al., 2009). The podiform chromitites form centimeters to meters scale
146 lenticular/tabular orebodies enclosed in thick dunite envelopes within mantle
147 harzburgites. The mantle harzburgites and dunites from Harmancık ophiolite have
148 been almost completely altered to serpentine and talc, and are unconformably overlain
149 by Neogene sedimentary units (e.g., Uysal et al., 2014, 2015).

150

151 **3. Petrography of dunites and chromitites**

152 In the Orhaneli ophiolite, dunites display adcumulate textures and consist of
153 mostly medium- to fine-grained olivine crystals with minor chromites (Fig. 3a, b).
154 Chromitites generally show adcumulus- to orthocumulus-like textures with euhedral

to subhedral chromite grains (Fig. 3c). They occur as bands and layers in dunites (Fig. 2a-c), and massive chromitites are very rare. The banded chromitite orebodies display schlieren textures, characterized by parallel layers of chromitite alternating with dunite (Fig. 2b). The thickness of the chromitite bands in the Orhaneli ophiolite typically ranges between 0.2 and 3 cm, rarely reaching up to 5 cm (Fig. 2b-c). In contrast, chromitites from the Harmancık mantle-crust transition zone occur as schlieren/bands, semi-massive, and disseminated textures. Chromite grains are mostly euhedral to subhedral. Dunites are made up predominantly of olivine (> 95%) and have a dominant cataclastic texture (Fig. 3d).

In the Orhaneli ophiolite, the mantle-crust transition zone is nearly horizontal (Fig. 2a), and we have selected 13 samples (dunites and chromitites) from the mantle-crust transition zone profile. The thickness of this profile is about 90 m and we fixed the base of the dunite as 0 m and its roof is +90 m. In the Harmancık ophiolite, 12 drill hole samples from the mantle-crust transition zone were selected for chemical analyses, owing to their pristine olivine grains. The drill hole samples including dunite and chromitite were collected from depths of 63.4 m to 73.4 m.

4. Analytical methods

4.1 Major oxide analysis of minerals

Major oxide compositions of olivine and chromite were determined by wavelength-dispersive X-ray spectrometry using a JEOL JXA8100 electron probe micro-analyzer at the Institute of Geology and Geophysics, Chinese Academy of

Sciences (IGGCAS). The analyses were carried out using an accelerating voltage of 15 kV, a 10 nA beam current, a 5 μm spot size and 10-30 s peak counting time. Natural and synthetic mineral standards were used for calibration. A ZAF procedure was used for matrix corrections. Typical analytical uncertainty for the analyzed elements was better than 1.5% (1RSD%).

4.2 Trace element analysis of olivine

In-situ trace element analyses of olivine were conducted on thin sections using a laser ablation inductively coupled plasma mass spectrometer (LA-ICP-MS) at IGGCAS. The LA-ICP-MS system consists of a 193 nm Coherent COMPex Pro ArF Excimer laser coupled to an Agilent 7500a ICP-MS. About 6-8 spots were measured for different olivine grains in each sample. The laser spot size was 140 μm, and the repetition rate was 8 Hz. Each analysis consisted of 60 s measurement of gas blank and 60 s ablation. The following isotopes were measured: ^{7}Li, ^{27}Al, ^{29}Si, ^{31}P, ^{39}K, ^{43}Ca, ^{45}Sc, ^{49}Ti, ^{51}V, ^{53}Cr, ^{59}Co, ^{66}Zn, ^{91}Zr, ^{163}Dy, ^{166}Er, ^{172}Yb. De Hoog et al. (2010) reported that potential interferences in olivine from matrix components MgO, SiO_2 and FeO, which are generated during ablation only and therefore unaccounted for by gas blank subtraction. The contribution of ^{26}Mg^{40}Ar to the ^{66}Zn signal is about 0.2 ppm, and the ^{29}Si^{16}O interference on ^{45}Sc accounted for 0.2 ppm of the signal (De Hoog et al., 2010), hence those are small enough to be ignored. A glass standard, NIST 610, was used for external calibration. For most of the trace elements NIST 612 standard was used to monitor instrument drift, and silicon (^{29}Si) was selected as an internal standard. The SiO_2 contents of NIST 610 and NIST 612 are 69.7% and 72.1%,

199 respectively. Reference values of NIST 610 and NIST 612 are from GeoREM
200 (http://georem.mpch-mainz.gwdg.de). The data were reduced using the GLITTER 4.0
201 program.

202 **4.3 Li concentration and isotope analyses of olivine**

203 In-situ analyses of Li concentrations and isotopic ratios of olivine were carried
204 out on gold-coated polished thin-sections using a Cameca IMS 1270 SIMS at the
205 Edinburgh Ion Microprobe Facility, in the University of Edinburgh, United Kingdom.
206 A $^{16}O_{2-}$ primary ion beam with an intensity of 12-16 nA was accelerated to 22.5 kV
207 and impacted onto the sample surface using Kohler illumination. The elliptical spot
208 area was approximately 20 × 30 μm. The secondary ion beam position in the field
209 aperture and the ^{7}Li peak position were automatically centered before each
210 measurement during a 60-s pre-sputter without beam rastering. Secondary ions were
211 counted in mono-collection, pulse-counting mode. Fifty cycles were measured with
212 counting times of 6 and 2.5 s for ^{6}Li and ^{7}Li, respectively. The count rate for ^{7}Li
213 ranged from 30,000 to 120,000 cps, depending on the Li concentration of the sample
214 and primary beam intensity, resulting in 1 s uncertainties of δ^{7}Li of 0.5-1.2‰.
215 Lithium concentrations were calculated using beam current corrected ^{7}Li count rates
216 of samples using 06JY34Ol as a standard (Li concentration = 1.73 ppm; Su et al.,
217 2015). The Li isotopic ratios are expressed as δ^{7}Li relative to the NIST L-SVEC
218 standard $\{\delta^{7}Li = [(^{7}Li/^{6}Li)_{sample}/(^{7}Li/^{6}Li)_{L\text{-}SVEC} - 1] \times 1000\}$. Basaltic standards
219 BCR2-G and ML3B-G were analyzed to monitor instrument drift, whereas 06JY34Ol
220 (δ^{7}Li = 3.1‰; Su et al., 2015) was used for calibration. Matrix composition (Fo

content) has an effect on measured olivine Li isotopic compositions; e.g., Su et al. (2015) showed that δ^7Li values increase by 1.0‰ for each mole percent decrease in the Fo content of olivine, and this was taken into account for calibration. As Fo contents of the olivines span a narrow range from 91.6 to 94.7, the matrix correction amounted to no more than 3‰, compared to a range of > 20‰ in δ^7Li for the whole dataset.

5. Results

5.1 Major oxide contents of minerals

Olivine in the Orhaneli and Harmancık dunites has Fo values of 92.4-94.0 and 91.6-93.5, respectively (Table S1; Fig. 4a-c). The chromitites contain olivine with somewhat higher Fo values (92.6-94.7 in Orhaneli; 93.3-94.4 in Harmancık) than those in the dunites (Table S1). The dunites from the two ophiolites have similar MnO (0.06-0.15 wt.%) and NiO (0.23-0.44 wt.%) contents in their olivine (Table S1). In the Orhaneli and Harmancık profile analyses, the variations of Mn concentrations in olivines are not continuous and yield abrupt change at the contact with chromitite layers. Compared to Mn, Ni concentrations show the reverse patterns (Fig. 5).

Chromite grains in dunites of the both ophiolites are generally uniform in TiO_2 contents (0.14-0.23 wt.% in Orhaneli; 0.11-0.22 wt.% in Harmancık), similar to those in the chromitites (0.14-0.26 wt.% and 0.13-0.22 wt.%), whereas their Cr# (100 × Cr/(Cr+Al)) and Mg# (100 × Mg/(Mg+Fe)) values are variable within ranges of 79.1-81.8 and 47.6-53.5 in the Orhaneli dunites, 70.6-80.2 and 41.9-52.9 in the

243 Harmancık dunites, 81.1-82.8 and 58.7-67.3 in the Orhaneli chromitites and 78.8-80.0
244 and 46.4-64.2 in the Harmancık chromitites (Table S2; Fig. 4).

245 **5.2 Trace element compositions of olivine**

246 From base to top, the mantle-crust transition zone in the Orhaneli ophiolite
247 includes many cyclic dunite and chromitite layers (Fig. 2a-b) with a total thickness of
248 90 m. Overall, olivines in chromitites show lower Co, Zn, Sc and V concentrations
249 than those in dunites (Fig. 5a, b). The Co concentrations of olivine in the dunites
250 (106-132 ppm in Orhaneli, 128-137 ppm in Harmancık) are higher than those of
251 primitive mantle (105 ppm; McDonough and Sun, 1995), whereas the concentrations
252 of Zn (6.0-44.8 ppm), Sc (2.14-3.68 ppm) and V (0.07-0.36 ppm) in all samples are
253 lower than primitive mantle (Zn: 55 ppm; Sc: 16.2 ppm; V: 82 ppm; McDonough and
254 Sun, 1995). The olivine in both dunites and chromitites from the two ophiolites has
255 lower incompatible trace element concentrations (Ti = 4.0-7.8 ppm, Zr = 0.010-0.034
256 ppm, and Yb = 0.007-0.027 ppm) than the counterparts in olivine phenocrysts in
257 MORB (Table S3; Fig. 6) (e.g., Piccardo et al., 2007; Foley et al., 2011). In the
258 Orhaneli section and Harmancık drill hole samples, there is no apparent correlation
259 between trace element compositions of olivine and the relative position of the layers
260 (Figs. 5, 6).

261 **5.3 Li concentrations and isotopic compositions**

262 In the Orhaneli dunites, olivine has Li concentrations varying from 0.9 to 1.5
263 ppm, and δ^7Li from 3.7 to 11.0‰ (Fig. 7), with no correlation between Li
264 concentrations and Li isotopic compositions (Fig. 8). In contrast, Li concentrations

(0.7 to 1.9 ppm) and δ^7Li values (-2.5 to 20.3‰) of olivine in the Harmancık dunites vary widely (Table S1), and the δ^7Li values are negatively correlated with the Li concentrations (Fig. 8). Most olivine grains in the two ophiolites show little change in Li concentrations and δ^7Li values from core to rim (Table S1). Nevertheless, different olivine grains in the same sample from Harmancık can have strongly variable Li isotopic compositions (up to 15‰ difference) (Table S1; Fig. 7). On the other hand, the chromitites from the two ophiolites display Li contents and δ^7Li values of olivine with 0.8 to 1.6 ppm and 5.0 to 14.7‰ in Orhaneli and 0.7 to 1.2 ppm and 4.1 to 15.6‰ in Harmancık (Table S1; Fig. 7).

6. Discussion

Based on trace elements and Li isotopes compositions of olivine in the dunites and chromitites from the mantle-crust transition zones for both ophiolites, we first evaluate the various processes that may account for the observed trace elemental and Li isotope variations, followed by models for the formation of dunites and chromitites.

6.1 Origin of mantle-crust transition zone dunites in the Orhaneli and Harmancık ophiolites

Dunite consists almost entirely of olivine and is usually formed by one of three processes (e.g., Su et al., 2016; Yao et al., 2018): 1) ultrahigh-degree partial melting of mantle with nearly all orthopyroxene being exhausted; 2) cumulate dunite left behind by the fractionation and accumulation of abundant olivine from an ultramafic-mafic

287 magma; 3) reaction between silica-undersaturated melt migrating in channels and
288 pyroxene-rich wall rock triggering the formation of replacive dunite.

289 Cumulate dunites are formed via crystal accumulation from magmas and
290 therefore olivine generally has low Fo (88-91) and feature a rapid decrease in the NiO
291 content with decreasing Fo (Santos et al., 2002; Song et al., 2007; Arai et al., 2012;
292 Seo et al., 2013; Su et al., 2016; Rospabé et al., 2018). Moreover, the coexisting
293 chromites show a wide range of Cr# from 15 to 76 as well as high TiO_2 contents (up
294 to 0.8 wt.%) (Santos et al., 2002; Song et al., 2007; Arai et al., 2012; Seo et al., 2013)
295 (Fig. 4a-c). In contrast, olivine in replacive dunites generally has higher Fo values (up
296 to 94), because the high-MgO melts reacting with peridotites convert olivine and
297 pyroxene in peridotite to high-Fo olivine (Rollinson et al., 2018). Besides, no obvious
298 correlation exists between the Fo and NiO of olivine grains within the replacive
299 dunites (Mazzucchelli et al., 2009). In the Orhaneli and Harmancık dunites, olivine
300 has higher Fo (91.6-94.0) and lower MnO contents (0.06-0.15 wt.%) than that from
301 cumulate dunites, while chromites display higher Cr# (79.1-82.8) and lower TiO_2
302 contents (0.14-0.26 wt.%) (Fig. 4c-d). These observations, together with the absence
303 of a clear correlation between Fo and NiO in olivine, demonstrate that the dunites
304 from both ophiolites could not be related to fractional crystallization (Fig. 4b). Instead,
305 all our data fall within the fields of replacive dunites (Fo: 90.4-94.6; MnO of olivine:
306 0.07-0.15 wt.%; Cr# of chromite: 23-89) (Suhr et al., 2003; Piccardo et al., 2007;
307 Ackerman et al., 2009; Mazzucchelli et al., 2009; Oh et al., 2012; Sanfilippo et al.,
308 2014, 2017) (Fig. 4), indicating that these dunites were formed by melt-peridotite

interaction rather than have a cumulate origin. Furthermore, although the olivines from these dunites show a good correlation between Ni and Mn, the correlation between Co and Mn is poor (Fig. 6b-c). According to olivine-melt partition coefficients (e.g., Beattie et al., 1991), Co and Ni are compatible in olivine, whereas Mn is incompatible, and hence segregation of olivine from its parental magma should produce a decrease of Co and Ni with increasing Mn (Sanfilippo et al., 2014). However, Co contents in olivine from the Orhaneli and Harmancık dunites are poorly correlated with Mn contents, and therefore incompatible with olivine fractionation and likely to be induced by melt migration.

For the Orhaneli and Harmancık ophiolites, the mineralogical and geochemical characteristics of mantle-crust transition zone dunites indicate that they were formed by melt-peridotite interaction: orthopyroxene + melt 1 → olivine + melt 2. In this reaction, melt 1 (reactant) is silica-undersaturated and melt 2 (product) is relatively enriched in SiO_2 and Cr_2O_3 due to progressive melt-rock reaction (e.g., Suhr, 1999; Zhou et al., 2005). Since the majority of all dunites are of refractory chemical nature and not akin to MORB (Figs. 4, 6), we argue that the reactant (melt 1) was highly depleted.

6.2 Origin of chromitites of the Orhaneli and Harmancık ophiolites

Olivines in Orhaneli and Harmancık chromitites have somewhat higher Fo than that contained in dunites, which likely implies an additional process for the chromitites. Subsolidus Mg-Fe exchange between olivine and chromite has been

usually reported in chromitites (e.g., Xiao et al., 2016):

$$FeSiO_4 + MgCr_2O_4 = MgSiO_4 + FeCr_2O_4 \quad \text{(Eq. 1)}$$

The Mg diffuses from chromite to olivine and Fe from olivine to chromite. The compositional effect of Fe-Mg exchange on olivine depends on the elemental contents and relative modal abundances of olivine and chromite in the rocks (Xiao et al., 2016). The Fe-Mg exchange effect on olivine in the dunites is negligible because of the extremely low amount of chromite. Recent studies (e.g., Qian et al., 2010) reported that despite differences in ionic size and charge, Sc and V diffuse at approximately similar rates to Mg, Fe and other divalent cations (e.g., Co and Zn). Cobalt and Zn are more compatible in chromite than in olivine, with crystal-melt partition coefficients from 8.3 to 2.1, and 7.9 to 3.6, respectively (https://earthref.org). Vanadium compatibility decreases in the order of chromite >> pyroxene >> olivine (Witt-Eickschen and O'Neill et al., 2005). In addition, the partitioning of Sc between chromite and olivine is strongly dependent upon the major element composition of chromite (Stosch et al., 1981). Thus, as expected, Co, Zn, Sc and V concentrations of olivine in the Orhaneli profile and Harmancık chromitites are lower than those in the associated dunites (Figs. 5a-b), which points to the relative modal abundances of chromite and olivine being a factor in determining the Sc, V, Co and Zn concentrations in olivine in chromitites (Xiao et al., 2016; Zhang et al., 2017). For example, in the Orhaneli profile, chromitite sample (+50 m) contains the highest modal amount of chromite and its olivine has the lowest Co, Zn, Sc and V concentrations (Fig. 5a).

353 Mantle-derived magmas generally have ca. 500 ppm Cr concentrations, whereas
354 the chromites derived from these melts contain 30-50 wt.% Cr_2O_3 (Zhou et al., 2014;
355 Zhang et al., 2017). During the evolution of magmatic systems, the oversaturation of
356 chromite in the magma is an important factor for the formation of chromitite. Addition
357 of silica to magmas has been widely accepted as a means of triggering chromite
358 precipitation, because SiO_2 addition can decrease Cr solubility (Irvine et al., 1986).
359 The increase in silica has been usually attributed to assimilation/reaction of more
360 siliceous materials or magma mixing (e.g., Arai et al., 2004; Zhou et al., 1994, 2014;
361 Zhang et al., 2017). In this regard, chromitites in the Orhaneli and Harmancık
362 mantle-crust transition zones are exclusively associated with dunites, and hence it is
363 unlikely that the oversaturation of chromite was caused by extensive assimilation of
364 siliceous-rich crust. Instead, the oversaturation of chromite induced by magma mixing
365 becomes the most likely scenario here. Mantle-derived mafic magma A rises through
366 the upper mantle and mixes with more Si-rich and Cr-rich magma (e.g., Lissenberg
367 and Dick, 2008), upon which the newly-formed, mixed magma B would move into
368 the field of chromite crystallization (Fig. 9). Additionally, the residual melt (melt 2)
369 following melt-peridotite reaction and orthopyroxene dissolution will also be enriched
370 with Cr and SiO_2 relative to the infiltrating melt (Arai and Yurimoto, 1995).
371 Therefore, it would further facilitate the oversaturation of chromite in the mixed
372 magma (Zhou et al., 1994, 2014; Su et al., 2019), driving crystallization of abundant
373 chromite and forming chromitite layers. Due to precipitation of chromite, mixed
374 magma ‘B’ would evolve to point ‘C’, i.e., back to the chromite-olivine cotectic line.

375

376 **6.3 Origin of infiltrating melts**

377 During melt-peridotite interaction, trace elements between minerals and melts
378 can be redistributed. The trace elements of olivine in the Orhaneli and Harmancık
379 dunites do not show any zoning (Tables S1, S3), indicating that they were fully
380 equilibrated with the percolating melts. Since dunites predominantly consist of olivine
381 grains, and other silicate minerals (e.g., pyroxene) are rare or absent, the trace element
382 concentrations of olivine cannot be affected by subsolidus re-equilibration among
383 silicate minerals. Thus, the olivine trace elements can be used to trace the composition
384 of the melt in chemical equilibrium with these crystals. The lower incompatible trace
385 element concentrations (Zr, Ti and HREE) in olivines from the Orhaneli and
386 Harmancık dunites relative to those of the olivines from the lower crustal sections of
387 ophiolites (Sanfilippo et al., 2014) (Fig. 6a) indicate that our dunites are not in
388 equilibrium with a melt derived from the lower oceanic crust. In addition, compared
389 to mantle harzburgites of the Orhaneli and Harmancık ophiolites (chromite Cr#: 43-55;
390 Fo < 91.6) (Uysal et al., 2017), the mantle-crust transition zone dunites have Cr# in
391 chromite of 79-82, NiO in olivine of 0.2-0.4 wt.% and Fo of 91.6-94.0, which are far
392 more refractory. The Mn and Co abundances of olivines in both the Orhaneli and
393 Harmancık dunites are lower than those of olivine phenocrysts within MORB
394 (Sobolev et al., 2007) (Fig. 6b-c), in conjunction with the lower trace-element
395 concentrations relative to primitive mantle (McDonough and Sun, 1995), suggesting
396 that these dunites were equilibrated with melts that are more depleted than MORB

(e.g., Piccardo et al., 2004; Sanfilippo and Tribuzio, 2011).

We can use the composition of the chromitites to put further constraints on the composition of its parental melts. In contrast to the incompatible elements, diffusion of compatible elements Cr, Al and Ti out of chromite is negligible (Abily and Ceuleneer, 2013), because Al and Ti enter olivine and/or serpentine in only very low amounts (e.g., Kamenetsky et al., 2001). As a consequence, we can use these elements to calculate the composition of equilibrated melts based on chromite compositions. The TiO_2 content of chromite is a key indicator of tectonic setting of where chromitite forms (e.g., Kamenetsky et al., 2001). The Orhaneli and Harmancık chromites have very low TiO_2, and plot in the arc or boninitic fields (Fig. 10a-b), suggesting crystallization from low-Ti island arc tholeiitic melts or boninitic melts. In addition, several studies have also shown that chromite compositions in chromitites reflect the composition of their parental melt (Kamenetsky et al., 2001; Rollinson, 2008; Zhou et al., 2014; Rollinson and Adetunji, 2015; Chen et al., 2019). The following equations were proposed by Rollinson and Adetunji (2015) to more closely reflect the empirical correlations defined by Kamenetsky et al. (2001) and applies to melt with an arc affinity:

$$(Al_2O_3)_{melt} = 5.2181 \times \ln(Al_2O_3)_{Chr} - 1.0505 \quad \text{(Eq. 2)}$$

$$(TiO_2)_{melt} = 1.0963 \times (TiO_2)_{Chr}^{0.7863} \quad \text{(Eq. 3)}$$

The implementation of equations (2) and (3) demonstrates that the melts in equilibrium with chromitite have the following composition: 9.8-10.8 wt.% Al_2O_3 and 0.23-0.38 wt.% TiO_2 in Orhaneli, and 10.7-11.4 wt.% Al_2O_3 and 0.22-0.33 wt.% TiO_2

in Harmancık. The inferred parental melts of the chromitites from the two ophiolites have similar Al_2O_3 and TiO_2 contents to boninitic melts (Fig. 10c), suggesting that the Orhaneli and Harmancık chromitites possibly originated in a forearc setting during the early stage of subduction. The zigzag pattern (Fig. 5) of the olivine trace element contents in the chromitites from the Orhaneli profile and Harmancık drill hole, in conjunction with the widespread occurrence of interlayered chromitites and dunites, could be the witness of multiple magma replenishments in the mantle-crust transition zone.

6.4 Lithium isotope constraints on the origin of Orhaneli and Harmancık dunites and chromitites

Due to the highly depleted composition of dunites and chromitites, traditional chemical indicators of tectonic setting can generally not be applied. However, Li isotope systematics of olivine may provide clues about the tectonic setting of the infiltrating melts. High-temperature partial melting is thought to induce negligible Li isotope fractionation (e.g., Tomascak et al., 1999; Ionov and Seitz, 2008) and Jeffcoate et al. (2007) estimated that the δ^7Li value of magmas generated by equilibrium melting would be < 0.5‰ different from their source. In addition, most studies have shown that Li isotopes do not fractionate during fractional crystallization of silicate magmas (e.g., Tomascak et al., 1999; Teng et al., 2006). Many studies also demonstrated that diffusion is an important mechanism controlling Li abundances and isotopic distribution (e.g., Su et al., 2014; Tomascak et al., 2016). Lithium

441 concentrations and isotopes do not show core-to-rim zoning in individual olivine
442 grains in most samples of the Orhaneli and Harmancık ophiolites (Table S2), and
443 chromite contains little or no Li (e.g., Jeffcoate et al., 2007; Chen et al., 2019). Thus,
444 the Li isotopic compositions of olivine have not been affected by inter-mineral
445 diffusion. Therefore, the Li isotopic compositions of olivines in the Orhaneli and
446 Harmancık dunites record the history of melt-rock interaction.

447 Compared to typical mantle peridotites with δ^7Li values of 2-6‰ and 1.0-1.8
448 ppm Li (Seitz and Woodland, 2000; Su et al., 2014), the olivines from the Orhaneli
449 dunites show a similar range of Li concentrations (0.9-1.5 ppm), but a slightly larger
450 range of δ^7Li values (+4.0 to +11.0‰) (Table S1; Figs. 7, 8), offset to higher values.
451 As the samples are relatively homogeneous (1s 0.8-1.7‰ based on multiple olivine
452 analyses in each sample) (Fig. 7) and the olivines are unzoned, these samples likely
453 reached Li isotope equilibrium during rock-melt interaction, and therefore could
454 reflect the composition of the infiltrating melt. Average δ^7Li per sample shows a more
455 restricted range from +4.8 to +8.7‰ with 1.1-1.3 ppm Li, suggesting reaction with
456 relatively homogeneous melt batches.

457 The Orhaneli chromitites have somewhat higher δ^7Li values (average δ^7Li per
458 sample +6.0 to +10.6‰ with 1.0-1.3 ppm), but the two samples with highest δ^7Li
459 shows considerable heterogeneity (based on multiple olivine analyses in each sample)
460 of > 4-7‰ even though individual olivines are unzoned. Excluding these samples, the
461 range of Orhaneli chromitites is +6.0 to +8.2‰, an even smaller range than the
462 dunites. These Li isotopic characteristics could be attributed to infiltrating melts in a

463 subduction zone setting. Dehydration of altered oceanic crusts during subduction can
464 induce that the Li isotope fractionation generates isotopically heavy-Li fluids and
465 light-Li slab residues (e.g., Elliott et al., 2004; Penniston-Dorland et al., 2017), but the
466 Li isotopic range of arc lavas (-1 to +12‰) reflects the heterogeneity of the altered
467 oceanic plate and overlying sediments (Tomascak et al., 2002; Elliott et al., 2004).
468 Mixing of various slab components and re-equilibration with Li already present in the
469 mantle wedge results in arc lavas with δ^7Li values that only slightly extend beyond
470 that of MORB. The dominance of δ^7Li values in the Orhaneli mantle-crust transition
471 zone that extends well beyond the MORB/mantle peridotite range point to a
472 ubiquitous subducting slab component present in the infiltrating melts. The survival of
473 these signatures suggests that the source of the interacting agent was rather shallow,
474 as Li isotopic signatures will re-equilibrate with ambient mantle at short length and
475 timescales (Halama et al., 2009). This is consistent with a subduction initiation.

476 Compared to Orhaneli, olivine from the Harmancık dunites shows much larger
477 δ^7Li variations of -2.5‰ up to +20.3‰, but also larger sample heterogeneity, with
478 only one sample having a ranging of δ^7Li of < 3‰ (Figs. 7, 8). The Harmancık
479 dunites were considerably more altered than the Orhaneli dunites, but the olivine
480 grains selected for Li isotope analyses were fresh and unzoned, and hence the
481 influences of alteration (such as serpentinization) on δ^7Li values between different
482 grains are likely to be small (e.g., Lundstrom et al., 2005). The larger range of δ^7Li
483 values in the Harmancık dunite may indicate the infiltrating melts with a wider range
484 of δ^7Li values, especially given that the slab-derived fluids and melts have a broad

485 range of compositions and are highly variable from one location to another (Elliott et
486 al., 2004; Yao et al., 2018). However, the heterogeneous distribution of δ^7Li in
487 individual samples from the Harmancık dunites and the negative correlation between
488 δ^7Li values and Li concentrations is indicative of incomplete diffusive equilibration
489 between olivines and infiltrating melts (Fig. 8) (e.g., Jeffcoate et al., 2007;
490 Penniston-Dorland et al., 2017), which is consistent with the studies of olivine Li
491 isotope of dunite from Trinity ophiolite (Lundstrom et al., 2005) and Luobusa
492 ophiolite (Su et al., 2016). Many studies have demonstrated that ^{6}Li diffuses about 2-3%
493 faster than ^{7}Li through melts and minerals (e.g., Lundstrom et al., 2005; Teng et al.,
494 2006). As Li diffuses from percolating melt into olivine, the δ^7Li of olivine will
495 become lower at first, but will then increase to higher values until δ^7Li equilibrates
496 with that of the infiltrating melt, due to equilibrium partitioning (Lundstrom et al.,
497 2005). During this process, temperature and time are the fundamental parameters that
498 control the efficiency of the isotopic exchange (Tomascak et al., 2016). We, therefore,
499 estimated the equilibration temperatures of the Harmancık and Orhaneli dunites and
500 chromitites based on the Al (Coogan et al., 2014) and Mg-Fe exchange (Ballhaus et
501 al., 1991) between olivine and chromite (Table 1). The Al-in-olivine thermometry
502 results (Coogan et al., 2014) show that the temperature range for Harmancık dunites
503 (933-979°C) is similar to that of the Orhaneli suite (960-993°C), while Mg-Fe
504 exchange temperatures (Ballhaus et al., 1991) are considerably lower: 714-778°C for
505 Orhaneli dunites and 663-755°C for Harmancık dunites. This suggests no significant
506 difference in temperature between Harmancık and Orhaneli ophiolites, so this cannot

explain the heterogeneity of the Harmancık samples. The main another factor of diffusion is time. Richter et al. (2014) found that very large lithium isotopic fractionations persisted after the lithium concentration had become effectively homogenized during diffusion process, suggesting that it still takes longer for the isotopic composition to become uniform compared to the time it takes for diffusion to homogenize the total lithium concentration. Thus, if infiltration of melts into the rocks occurred shortly before obduction and exhumation, Li isotopes would not fully equilibrate, and isotope heterogeneity would be preserved during relatively rapid cooling. Heterogeneities in the Harmancık samples could indicate rapid cooling was essential to preserve the observed isotope heterogeneities.

In summary, excluding two heterogeneous samples (Fig. 7), the Li isotope signatures of olivine in dunites and chromitites from the Orhaneli ophiolite are likely primary features inherited from their parental melts, with all olivines falling between δ^7Li values of +5‰ and +9‰, which is within the range of arc lavas but isotopically heavier than MORB (Fig. 7) (Chan et al., 2002; Tomascak et al., 2002), suggesting an affinity with arc magmatism. The olivine Li isotopic compositions of Harmancık mantle-crust transition zone chromitites are similar to those from Orhaneli, but still, likely have diffusional heterogeneities due to incomplete equilibration between infiltrating melt and olivine. Nevertheless, their average compositions (+6 to +11‰) does suggest a melt source similar to the one that crystallized Orhaneli chromitites.

The estimated Al_2O_3 and TiO_2 contents of the parental magmas of chromitites in the two ophiolites are similar to the signatures of boninitic melts. Given that boninitic

529 magmas have been widely found in preserved fore-arcs related to subduction
530 initiation (e.g., Reagan et al., 2017; Stern et al., 2012), this suggests that the Orhaneli
531 and Harmancık ophiolites possibly originated in a subduction initiation setting, which
532 gives additional support to studies suggesting that these settings represent an ideal
533 environment for forming ophiolites with economically viable chromitite deposits
534 (Johnson, 2012).
535
536 **7 Conclusions**
537 This study presents in-situ trace elements and Li isotopic compositions of olivine
538 in dunites and chromitites from the Orhaneli and Harmancık mantle-crust transition
539 zone. The following conclusions can be drawn:
540 1. Compared to olivine from cumulate dunites, the olivine in the Orhaneli and
541 Harmancık dunites is distinct by higher Ni, lower Mn concentrations and extreme
542 depletion of incompatible trace elements (Ti, Zr and HREE), which are consistent
543 with the formation of dunites driven by interaction of peridotite with depleted
544 melts.
545 2. The relatively uniform Li isotopic compositions (+4 to +11‰) of olivines from
546 Orhaneli dunites indicate these samples reached Li isotope equilibrium, and
547 suggest a reaction driven by relatively homogeneous melt batches with a
548 subduction component, whereas the large δ^7Li variations (-2.5 to +20.3‰) in
549 olivine from Harmancık dunites reflect incomplete diffusive equilibration during
550 the melt percolation through these dunites.

3. The formation of chromitites in the mantle-crust transition zone of the two ophiolites was likely triggered by the magma mixing. The calculated Al_2O_3 (9.8-11.4 wt.%) and TiO_2 (0.22-0.38 wt.%) contents of the parental magmas of chromitites demonstrate a boninite-like geochemical affinity, i.e., a subduction initiation setting, which is in good agreement with the Li isotopic compositions of their olivines.
4. In contrast to the dunites, the higher Fo contents of olivine in the chromitites could be caused by the Mg-Fe exchange between olivine and chromite. The lower Sc, V, Co and Zn concentrations of olivine in the chromitites are controlled by the modal abundances of chromite.

Acknowledgements

This paper benefited from constructive and detailed comments of two anonymous reviewers, and efficient editorial handling by Xian-Hua Li. This study was supported by the National Natural Science Foundation of China (Grants 91755205 and 41772055), and by a Visiting Student grant to Chen Chen from the United Kingdom National Environment Research Council 'Deep Volatiles' program (Grant NE/M000427/1). We thank Wei Lin, Yang Chu and Jie-Jun Jing for the assistance in the field trips in the Kızıldağ.

References

Abily, B., Ceuleneer, G., 2013. The dunitic mantle-crust transition zone in the Oman ophiolite: residue of melt-rock interaction, cumulates from high-MgO melts, or

573 both? Geology 41, 67-70.
574 Ackerman, L., Jelínek, E., Medaris Jr., G., Ježek, J., Siebel,W., Strnad, L., 2009.
575 Geochemistry of Fe-rich peridotites and associated pyroxenites from Horní Bory,
576 Bohemian Massif: insights into subduction-related melt-rock reactions. Chemical
577 Geology 259, 152-167.
578 Anders, E., Ebihara, M., 1982. Solar system abundances of the elements. Geochimica
579 et Cosmochimica Acta 46, 2363-2380.
580 Arai, S., Ishimaru, S., Mizukami, T., 2012. Methane and propane micro-inclusions in
581 olivine in titanoclinohumite-bearing dunites from the Sanbagawa high-P
582 metamorphic belt, Japan: hydrocarbon activity in a subduction zone and Timobility.
583 Earth and Planetary Science Letters 354, 1-11.
584 Arai, S., Yurimoto, H., 1995. Possible sub-arc origin of podiform chromitites. Island
585 Arc 4, 104-111.
586 Arai, S., Uesugi, J., Ahmed, A.H., 2004. Upper crustal podiform chromitite from the
587 northern Oman ophiolite as the stratigraphically shallowest chromitite in ophiolite
588 and its implication for Cr concentration. Contributions to Mineralogy and Petrology
589 147, 145-154.
590 Ballhaus, C., 1998. Origin of podiform chromite deposits by magma mingling. Earth
591 and Planetary Science Letters 156, 185-193.
592 Ballhaus, C., Berry, R.F., Green, D.H., 1991. High pressure experimental calibration
593 of the olivine-orthopyroxene-spinel oxygen geobarometer: implications for the
594 oxidation state of the upper mantle. Contributions to Mineralogy and Petrology 107,

595 27-40.
596 Beattie P., Ford, C., Russell, D., 1991. Partition coefficients for olivine-melt and
597 orthopyroxene-melt systems. Contributions to Mineralogy and Petrology 109,
598 212-224.
599 Chan, L.H., Alt, J.C., Teagle, D.A.H., 2002. Lithium and lithium isotope profiles
600 through the upper oceanic crust: a study of seawater-basalt exchange at ODP Sites
601 504B and 896A. Earth and Planetary Science Letters 201, 187-201.
602 Chen, C., Su, B.X., Xiao, Y., Pang, K.N., Robinson, P.T., Uysal, İ., Lin, W., Qin, K.Z.,
603 Avcı, E., Kapsiotis, A., 2019. Intermediate chromitite in Kızıldağ ophiolite (SE
604 Turkey) formed during subduction initiation in Neo-Tethys. Ore Geology Reviews
605 104, 88-100.
606 Chen, C., Su, B.X., Xiao, Y., Lin, W., Chu, Y., Liu, X., Bai, Y., 2018. Geological
607 records of subduction initiation of Neo-Tethyan ocean: ophiolites and metamorphic
608 soles in southern Turkey. Acta Petrologica Sinica 34, 3302-3314 (in Chinese with
609 English abstract).
610 Coogan, L.A., Saunders, A.D., Wilson, R.N., 2014. Aluminum-in-olivine
611 thermometry of primitive basalts: evidence of an anomalously hot mantle source
612 for large igneous provinces. Chemical Geology 368, 1-10.
613 De Hoog, J.C.M., Gall, L., Cornell, D.H., 2010. Trace-element geochemistry of
614 mantle olivine and application to mantle petrogenesis and geothermobarometry.
615 Chemical Geology 270, 196-215.
616 Derbyshire, E.J., O'Driscoll, B., Lenaz, D., Gertisser, R., Kronz, A., 2013.

617 Compositionally heterogeneous podiform chromitite in the Shetland ophiolite
618 complex (Scotland): Implications for chromitite petrogenesis and late-stage
619 alteration in the upper mantle portion of a supra-subduction zone ophiolite. Lithos
620 162, 279-300.
621 Dilek, Y., Thy, P., 2006. Age and petrogenesis of plagiogranite intrusions in the
622 Ankara mélange, Central Turkey. Island Arc 15, 44-57.
623 Elliott, T., Jefcoate,A., Bouman, C., 2004. The terrestrial Li isotope cycles:
624 light-weight constraints on mantle convection. Earth and Planetary Science Letters
625 220, 231-245.
626 Foley, S.F., Prelevic, D., Rehfeldt, T., Jacob, D.E., 2013. Minor and trace elements in
627 olivines as probes into early igneous and mantle melting processes. Earth and
628 Planetary Science Letters 363, 181-191.
629 Foley, S.F., Jacob, D.E., O'Neill, H.S.C., 2011. Trace element variations in olivine
630 phenocrysts from Ugandan potassic rocks as clues to the chemical characteristics of
631 parental magmas. Contributions to Mineralogy and Petrology 162, 1-20.
632 Halama, R., Savov, I.P., Rudnick, R.L., McDonough, W.F., 2009. Insights into Li and
633 Li isotope cycling and sub-arc metasomatism from veined mantle xenoliths,
634 Kamcharka. Contributions to Mineralogy and Patrology 158, 197-222.
635 Ionov, D.A., Seitz, H.M., 2008. Lithium abundances and isotopic compositions in
636 mantle xenoliths from subduction and intra-plate settings: mantle sources vs.
637 eruption histories. Earth and Planetary Science Letters 266, 316-331.
638 Irvine, T.N., Sharpe, M.R., Gallagher, M.L., 1986. Magma mixing and the origin of

639 stratiform oxide ore zones in the Bushveld and Stillwater complexes. Metallogeny
640 of Basic and Ultrabasic Rocks, 183-198.
641 Jeffcoate, A.B., Elliott, T., Kasemann, S.A., Ionov, D., Cooper, K., Brooker, R., 2007.
642 Li isotope fractionation in peridotites and mafic melts. Geochimica et
643 Cosmochimica Acta 71, 202-218.
644 Johnson, C., 2012. Podiform chromite at Voskhod, Kazakhstan. Unpublished PhD
645 Thesis. Cardiff University. http://orca.cf.ac.uk/40714/
646 Kamenetsky, V.S., Crawford, A.J., Meffre, S., 2001. Factors controlling chemistry of
647 magmatic spinel: an empirical study of associated olivine, Cr-spinel and melt
648 inclusions from primitive rocks. Journal of Petrology 42, 655-671.
649 Lissenberg, C.J., Dick, H.J.B., 2008. Melt-rock reaction in the lower oceanic crust and
650 its implications for the genesis of mid-ocean ridge basalt. Earth and Planetary
651 Science Letters 271, 311-325
652 Lundstrom, C.C., Chaussidon, M., Hsui, A.T., Kelemen, P., Zimmerman, M., 2005.
653 Observations of Li isotopic variations in the Trinity Ophiolite: evidence for isotopic
654 fractionation by diffusion during mantle melting. Geochimica et Cosmochimica
655 Acta 69, 735-751.
656 Mazzucchelli, M., Rivalenti, G., Brunelli, D., Zanetti, A., Boari, E., 2009. Formation
657 of highly refractory dunite by focused percolation of pyroxenite-derived melt in the
658 Balmuccia Peridotite Massif (Italy). Journal of Petrology 50, 1205-1233.
659 McDonough, W.F., Sun, S.S., 1995. The composition of the Earth. Chemical Geology
660 20, 223-253.

661 Oh, C.W., Seo, J., Choi, S.G., Rajesh, V.J., Lee, J.H., 2012. U-Pb SHRIMP zircon
662 geochronology, petrogenesis, and tectonic setting of the Neoproterozoic Baekdong
663 ultramafic rocks in the Hongseong Collision Belt, South Korea. Lithos 131,
664 100-112.
665 Paktunc, A.D., 1990. Origin of podiform chromite deposits by multistage melting,
666 melt segregation and magma mixing in the upper mantle. Ore Geology Reviews 5,
667 211-222.
668 Pearce, J.A., Barker, P.F., Edward, S.J., Parkinson, I.J., Leat, P.T., 2000. Geochemistry
669 and tectonic significance of peridotites from the south Sandwich arc-basin system,
670 south Atlantic. Contributions to Mineralogy and Petrology 139, 36-53.
671 Peighambari, S., Uysal, İ., Stosch, H.G., Ahmadipour, H., Heidarian, H., 2016.
672 Genesis and tectonic settings of ophiolitic chromitites from the Dehsheikh
673 ultramafic complex (Kerman, southeastern Iran): inferences from platinum-group
674 elements and chromite compositions. Ore Geology Reviews 74, 39-51.
675 Penniston-Dorland, S., Liu, X.M., Rudnick, R.L., 2017. Lithium isotope geochemistry.
676 Reviews in Mineralogy and Geochemistry 82, 165-217.
677 Piccardo, G.B., Zanetti, A., Muntener, O., 2007. Melt/peridotite interaction in the
678 Southern Lanzo peridotite: field, textural and geochemical evidence. Lithos 94,
679 181-209.
680 Piccardo, G.B., Müntener, O., Zanetti, A., Pettke, T., 2004. Ophiolitic peridotites of
681 the Alpine-Apennine system: mantle processes and geodynamic
682 relevance. International Geology Review 46, 1119-1159.

683 Qian, Q., O'Nell, H.S.C., Hermann, J., 2010. Comparative diffusion coefficients of
684 major and trace elements in olivine ~950°C from a xenocryst included in dioritic
685 magma. Geology 4, 331-334.
686 Rampone, E., Borghini, G., Godard, M., Ildefonse, G., Cridpini, L., Fumagalli, P.,
687 2016. Melt/rock reaction at oceanic peridotite/gabbro transition as revealed by trace
688 element chemistry of olivine. Geochemica et Cosmochimica Acta 190, 309-331.
689 Reagan, M.K., Pearce, J.A., Petronotis, K., Almeev, R.R., Avery, A.J., Carvallo, C.,
690 Chapman, T., Christeson, G.L., Ferré, E.C., Godard, M., Heaton, D.E., Kirchenbaur,
691 M., Kurz, W., Kutterolf, S., Li, H.Y., Li, Y.B., Michibayashi, K., Morgan, S.,
692 Nelson, W.R., Prytulak, J., Python, M., Robertson, A.H.F., Ryan, J.G., Sager, W.W.,
693 Sakuyama, T., Shervais, J.W., Shimizu, K, Whattam, S.A., 2017. Subduction
694 initiation and ophiolite crust: new insights from IODP drilling. International
695 Geology Review 59, 1439-1450.
696 Richter, F., Watson, B., Chaussidon, M., Mendybaev, R., Ruscitto, D., 2014. Lithium
697 isotope fractionation by diffusion in minerals. Part I: pyroxenes. Geochimica et
698 Cosmochimica Acta 126, 352-370.
699 Rollinson, H., Mameri, L., Barry, T., 2018. Polymineralic inclusion in mantle
700 chromitites from the Oman ophiolite indicate a highly magnesian parental melt.
701 Lithos 310, 381-391.
702 Rollinson, H., Adetunji, J., 2015. The geochemistry and oxidation state of podiform
703 chromitites from the mantle section of the Oman ophiolite: a review. Gondwana
704 Research 27, 543-554.

Rollinson, H., 2008. The geochemistry ofmantle chromitites from the northern part of the Oman ophiolite: inferred parental melt composition. Contributions to Mineralogy and Petrology 156, 273-288.

Rospabé, M., Benoit, M., Ceuleneer, G., Hodel, F., Kaczmarek, M.A., 2018. Extreme geochemical variability through the dunitic transition zone of the Oman ophiolite: implications for melt/fluid reactions at Moho level beneath oceanic spreading centres. Geochimica Cosmochimica Acta 234, 1-23.

Rudnick, R.L., Ionov, D.A., 2007. Lithium elemental and isotopic disequilibrium in minerals from peridotite xenoliths from far-east Russia: product of recent melt/ fluid-rock reaction. Earth and Planetary Science Letters 256, 278-293.

Sanfilippo, A., Tribuzio, R., Ottolini, L., Hamada, M., 2017. Water, lithium and trace element compositions of olivine from Lanzo South replacive mantle dunite (western Alps): new constraints into melt migration processes at cold thermal regimes. Geochimica et Cosmochimica Acta 214, 51-72.

Sanfilippo, A., Tribuzio, R., 2011. Melt transport and deformation history in a non-volcanic ophiolitic section northern Apennine, Italy: implications for crustal accretion at slow spreading settings. Geochemistry, Geophysics, Geosystems 12, Q0AG04.

Santos, J.F., Schärer, U., Ibarguchi, J.I.G., Girardeau, J., 2002. Genesis of pyroxenite-rich peridotite at Cabo Ortegal (NW Spain): geochemical and Pb-Sr-Nd isotope data. Journal of Petrology 43, 17-43.

726 Sarıfakıoğlu, E., Dilek, Y., Sevin, M., 2017. New synthesis of the
727 Izmir-Ankara-Erzincan suture zone and the Ankara mélange in northern Anatolia
728 based on new geochemical and geochronological constraints. Geological Society of
729 America Special paper 525, 1-62.
730 Sarıfakıoğlu, E., Ozen, H., Winchester, J.A., 2009. Whole rock and mineral chemistry
731 of ultramafic-mafic cumulates from the Orhaneli (Bursa) ophiolite, NW Anatolia.
732 Turkish Journal of Earth Sciences 18, 55-83.
733 Seitz, H.M., Woodland, A.B., 2000. The distribution of lithium in peridotitic and
734 pyroxenitic mantle lithologies - an indicator of magmatic and metasomatic
735 processes. Chemical Geology 166, 47-64.
736 Seo, J., Oh, C.W., Choi, S.G., Rajesh, V.J., 2013. Two ultramafic rock types in the
737 Hongseong area, south Korea: tectonic significance for northeast Asia. Lithos 176,
738 30-39.
739 Sobolev, A.V., Hofmann, A.W., Kuzmin, D.V., Yaxley, G.M., Arndt, N.T., Chung, S.L.,
740 Danyushevsky, L.V., Elliott, T., Frey, F.A., Garcia, M.O., Gurenko, A.A.,
741 Kamenetsky, V.S., Kerr, A.C., Krivolutskaya, N.A., Matvienkov, V.V., Nikogosian,
742 I.K., Rocholl, A., Sigurdsson, I.A., Sushchevskaya, N.M., Teklay, M., 2007. The
743 amount of recycled crust in sources of mantle-derived melts. Science 316, 412-417.
744 Song, S.G., Su, L., Niu, Y.L., Zhang, L.F., Zhang, G.B., 2007. Petrological and
745 geochemical constraints on the origin of garnet peridotite in the North Qaidam
746 ultrahigh-pressure metamorphic belt, northwestern China. Lithos 96, 243-265.

747 Stern, R.J., Reagan, M., Ishizuka, O., Ohara, Y., Whattam, S., 2012. To understand
748 subduction initiation, study forearc crust: to understand forearc crust, study
749 ophiolites. Lithosphere 4, 469-483.
750 Stosch, H.G., 1981. Sc, Cr, Co and Ni partitioning between minerals from spinel
751 peridotite xenoliths. Contributions to Mineralogy and Petrology 78, 166-174.
752 Suhr, G., Hellebrand, E., Snow, J.E., Seck, H.A., Hofmann, A.W., 2003. Significance
753 of large, refractory duninte bodies in the upper mantle of the Bay of Island
754 ophiolite. Geochemistry, Geophysics, Geosystems 4.
755 Suhr, G., 1999. Significance of upper mantle hosted dunite bodies for melt migration
756 and extraction under oceanic spreading centres: inferences from reactive transport
757 modelling. Journal of Petrology 40, 575-599.
758 Su, B.X., Zhou, M.F., Jing, J.J., Robinson, P., Chen, C., Xiao, Y., Liu, X., Shi, R.D.,
759 Lenaz, D., Hu, Y., 2019. Distinctive melt activity and chromite mineralization in
760 Luobusa and Purang ophiolites, southern Tibet: constraints from trace element
761 compositions of chromite and olivine. Science Bulletin 64, 108-121.
762 Su, B.X., Zhou, M.F., Robinson, P.T., 2016. Extremely large fractionation of Li
763 isotopes in a chromitite-bearing mantle sequence. Scientific Reports 6, 22370.
764 Su, B.X., Gu, X.Y., Deloule, E., Zhang, H.F., Li, Q.L., Li, X.H., Vigier, N., Tang,
765 Y.J., Tang, G.Q., Liu, Y., Brewer, A., Mao, Q., Ma, Y.G., 2015. Potential
766 orthopyroxene, clinopyroxene and olivine reference materials for in-situ lithium
767 isotope determination. Geostandards and Geoanalytical Research 39, 357-369.

768 Su, B.X., Zhang, H.F., Deloule, E., Vigier, N., Hu, Y., Tang, Y.J., Xiao, Y., Sakyi,
769 P.A., 2014. Distinguish silicate and carbonatite mantle metasomatism by using
770 lithium and its isotopes. Chemical Geology 381, 67-77.
771 Tankut, A., 1980. The Orhaneli massif, Turkey ophiolites. Geological Survey
772 Department Nicosia, 702-713.
773 Teng, F.Z., McDonough, W.F., Rudnick, R.L., Walker, R.J., Sirbescu, M.L.C., 2006.
774 Lithium isotopic systematics of granites and pegmatites from the Black Hills, South
775 Dakota. American Mineralogist 91, 1488-1498.
776 Tomascak, P.B., Magna, T., Dohmen, R., 2016. Advances in Lithium Isotope
777 Geochemistry. Springer International Publishing Switzerland, 1-195.
778 Tomascak, P.B., Tera, F., Helz, R.T., Walker, R.J., 1999. The absence of lithium
779 isotope fractionation during basalt differentiation: new measurements by
780 multicollector sector ICP-MS. Geochimica et Cosmochimica Acta 63, 907-910.
781 Tomascak, P.B., Langmuir, C.H., le Roux, P.J., Shirey, S.B., 2008. Lithium isotopes
782 in global mid-ocean ridge basalts. Geochimica et Cosmochimica Acta 72,
783 1626-1637.
784 Tomascak, P.B., Widom, E., Benton, L.D., Goldstein, S.L., Ryan, J.G., 2002. The
785 control of lithium budgets in island arcs. Earth and Planetary Science Letters 196,
786 227-238.
787 Uysal, İ., Dokuz, A., Kapsiotis, A., Saka, S., Karslı, O., Kaliwoda, M., Müller, D.,
788 2017. Petrogenesis of ultramafic rocks from the eastern Orhaneli ophiolite, NW
789 Turkey: hints on the initiation and evolution of melt-peridotite interaction processes

790 within a heterogeneously depleted mantle section. Journal of Asian Earth
791 Sciences 148, 51-64.
792 Uysal, İ., Akmaz, R.M., Kapsiotis, A., Demir, Y., Saka, S., Avcı, E., Muller, D., 2015.
793 Genesis and geodynamic significance of chromitites from the Orhaneli and
794 Harmancik ophiolites (Bursa, NW Turkey) as evidenced by mineralogical and
795 compositional data. Ore Geology Reviews 65, 26-41.
796 Uysal, İ., Şen, A.D., Ersoy, E.Y., Dilek, Y., Saka, S., Zaccarini, F., Escayola, M.,
797 Karslı, O., 2014. Geochemical make-up of oceanic peridotites from NW Turkey
798 and the multi-stage melting history of the Tethyan upper mantle. Mineralogy and
799 Petrology 108, 49-69.
800 Vlastelic, I., Koga, K., Chauvel, C., Jacques, G., Telouk, P., 2009. Survival of lithium
801 isotopic heterogeneities in the mantle supported by HIMU-lavas from Rurutu Island,
802 Austral Chain. Earth and Planetary Science Letters 286, 456-466.
803 Witt-Eickschen, G., O'Neill, H.S.C., 2005. The effect of temperature on the
804 equilibrium distribution of trace elements between clinopyroxene, orthopyroxene,
805 olivine and spinel in upper mantle peridotite. Chemical Geology 221, 65-101.
806 Xiao, Y., Teng, F.Z., Su, B.X., Hu, Y., Zhou, M.F., Zhu, B., Shi, R.D., Huang, Q.S.,
807 Gong, X.H. He, Y.S., 2016. Iron and magnesium isotopic constraints on the origin
808 of chemical heterogeneity in podiform chromitite from the Luobusa ophiolite, Tibet.
809 Geochemistry, Geophysics, Geosystems 17, 940- 953.
810 Yao, Z.S., Qin, K.Z., Mungall, J.E., 2018. Tectonic controls on Ni and Cu contents of
811 primary mantle-derived magmas for the formation of magmatic sulfide deposits.

812 American Mineralogist 103, 1545-1567.
813 Zhang, P.F., Zhou, M.F., Su, B.X., Uysal, İ., Robinson, P.T., Avcı, E., He, Y.S., 2017.
814 Iron isotopic fractionation and origin of chromitites in the paleo-Moho transition
815 zone of the Kop ophiolite, NE Turkey. Lithos 268, 65-75.
816 Zhou, M.F., Robinson, P.T., Su, B.X., Gao, J.F., Li, J.W., Yang, J.S., Malpas, J., 2014.
817 Compositions of chromite, associated minerals, and parental magmas of podiform
818 chromite deposits, the role of slab contamination of asthenospheric melts in
819 suprasubduction zone environments. Gondwana Research 26, 262-283.
820 Zhou, M.F., Robinson, P.T., Malpas, J., Edwards, S., Qi, L., 2005. REE and PGE
821 geochemical constraints on the formation of dunites in the Luobusa ophiolite,
822 southern Tibet. Journal of Petrology 46, 615-639.
823 Zhou, M.F., Robinson, P.T., Bai, W., 1994. Formation of podiform chromitites by
824 melt/rock interaction in the upper mantle. Mineralium Deposita 29, 98-101.
825

826 **Figure Captions:**

827 Fig. 1 (a) Map showing distribution of the continental blocks, major sutures and
828 related ophiolites in the Eastern Mediterranean region (modified after Chen et al.,
829 2018). (b) Simplified geological map of the Orhaneli and Harmancık ophiolites (after
830 Uysal et al., 2015). Red stars in (b) are the sampling locations. IASZ: Izmir-Ankara
831 Suture Zone; ITSZ: Inner-Tauride Suture Zone; BZSZ: Bitlis-Zagros Suture Zone.

832

833 Fig. 2 Photographs of field sites with numbered sampling locations and hand
834 specimens of dunites and chromitites from the Orhaneli mantle-crust transition zone.

835 (a) Banded chromitites that occur by the rhythmic layering of chromitite and dunite.
836 (b) Banded chromitite. (c) Disseminated chromitite.
837
838 Fig. 3 Back scattered electron images of thin sections of dunites and chromitites from
839 the Orhaneli (a)-(c) (sample Ol-1, 2-2 and 4-2) and Harmancık (d) (sample 71.5 m)
840 ophiolites.
841
842 Fig. 4 Plots of (a) MnO vs. Fo of olivine, (b) NiO vs. Fo of olivine, (c) Cr# of
843 chromite vs. Fo, and (d) Cr# vs. TiO_2 of chromite in dunites from the Orhaneli and
844 Harmancık ophiolites. The gray and pink fields represent literature olivine/chromite
845 composition ranges of cumulate dunites and dunites formed by peridotite-melt
846 interaction, respectively. The cumulate dunite field is defined using data from Santos
847 et al. (2002), Song et al. (2007), Arai et al. (2012) and Seo et al. (2013). The replacive
848 dunite field is defined using data from Suhr et al. (2003), Piccardo et al. (2007),
849 Ackerman et al. (2009), Mazzuchelli et al. (2009), Oh et al. (2012), Sanfilippo et al.
850 (2014, 2017).
851
852 Fig. 5 Elemental (Fo, Ni, Mn, Li, Co, Zn, Sc and V) and isotopic (δ^7Li) variations of
853 olivine compositions in the Orhaneli profile (a) and Harmancık drill hole (b). Olivine
854 grains from dunites are shown as blue circles, whereas pink circles are olivine grains
855 from chromitites. Scanned photographs of dunites and chromitites are shown to
856 clearly describe the effect of chromite proportion on olivine trace element

857 compositions.

858

859 Fig. 6 (a) Primitive mantle-normalized pattern of olivine in the dunites from Orhaneli
860 and Harmancık ophiolites. Plots of (b) Ni (ppm) vs. Mn (ppm), (c) Co (ppm) vs. Mn
861 (ppm) of olivine in the dunites from the two ophiolites. Primitive mantle values are
862 from Anders and Ebihara (1982). Compositions of lower crust data in (a) are from
863 Sanfilippo et al. (2014, 2017) and Rampone et al. (2016). The compositions of olivine
864 phenocrysts in MORB are from Sobolev et al. (2007).

865

866 Fig. 7 Li isotopic compositions of olivines in dunite and chromititesfrom the Orhaneli
867 and Harmancık ophiolites. The δ^7Li range of MORB is from Tomascak et al. (2008),
868 and the δ^7Li range of arc lava is from Tomascak et al. (2002) and Chan et al. (2002).

869

870 Fig. 8 Diagram of δ^7Li vs. Li of olivine in the Orhaneli and Harmancık dunites. The
871 arrow is the trend of Li diffusion during melt-rock interaction (after Lundstrom et al.
872 (2005)).

873

874 Fig. 9 A petrologic model for chromitite formation in the Orhaneli and Harmancık
875 ophiolites in the simplified system olivine (Ol) - quartz (Q) - chromite (Chr). The
876 trends in the phase diagrams are after Zhou et al. (1994) and Zhang et al. (2017).

877

878 Fig. 10 (a) TiO_2 vs. Al_2O_3 (after Kamenetsky et al., 2001 and Derbyshire et al., 2013),

(b) Cr# vs. TiO_2 (after Pearce et al., 2000) of chromite in the chromitites and (c) TiO_2 vs. Al_2O_3 (after Peighambari et al., 2016) of parental melts for the Orhaneli and Harmancık chromitites. FMM: fertile MORB mantle. The subscripts b and I represent boninite and island arc tholeiite, respectively. BON: boninite; IAT: island arc tholeiite; MORB: mid-ocean ridge basalt. Data of grey hexagons, triangles and circles representing lherzolite, harzburgite and dunite, respectively, are from Uysal et al. (2014).

Figure

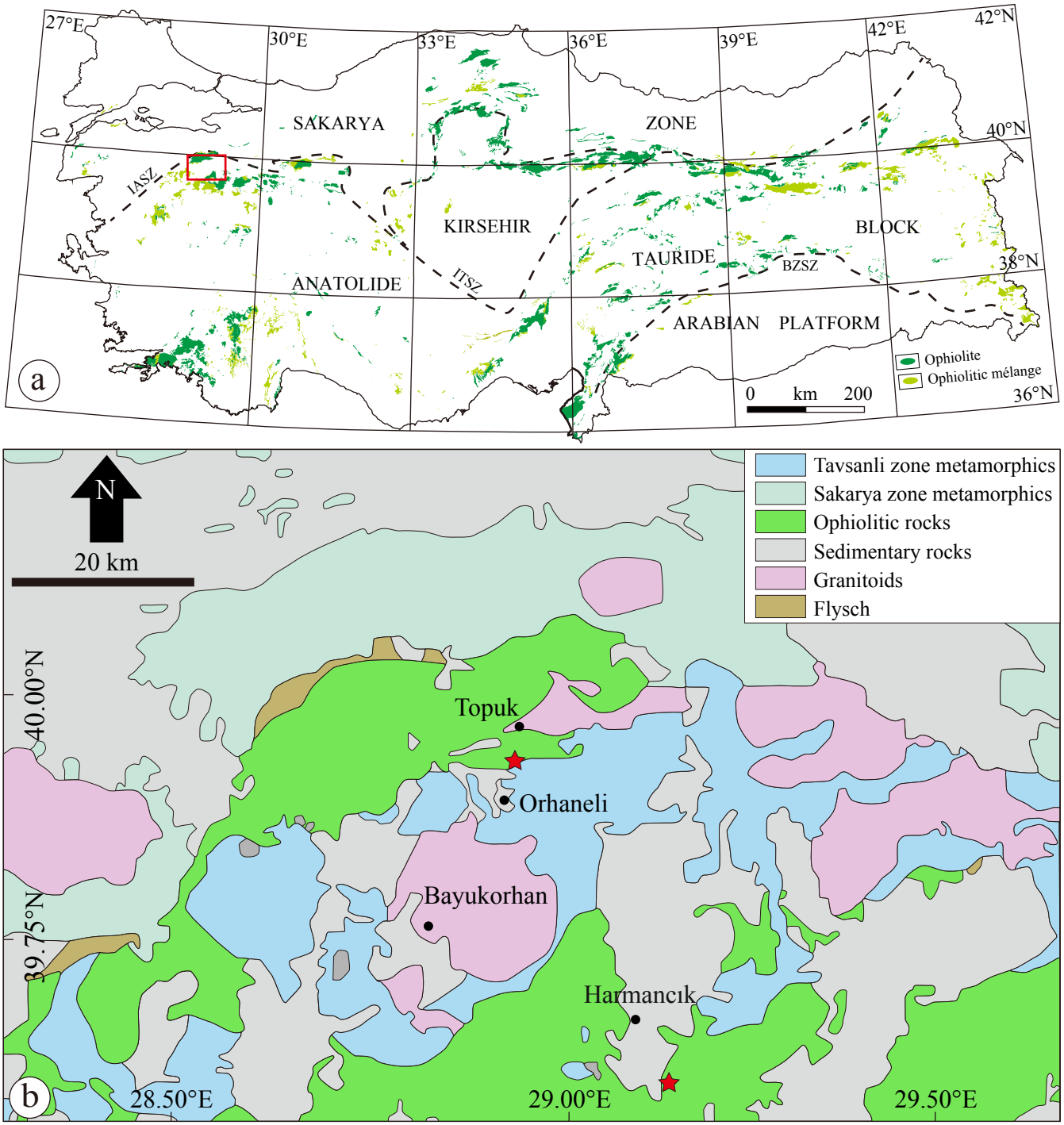
27°E
30°E
33°E
36°E
39°E
42°E
42°N
40°N
38°N
36°N
SAKARYA
ZONE
IASZ
KIRSEHIR
BLOCK
TAURIDE
BZSZ
ANATOLIDE
ITSZ
ARABIAN PLATFORM
a
Ophiolite
Ophiolitic mélange
0 km 200
N
20 km
Tavsanli zone metamorphics
Sakarya zone metamorphics
Ophiolitic rocks
Sedimentary rocks
Granitoids
Flysch
40.00°N
39.75°N
Topuk
Orhaneli
Bayukorhan
Harmancık
b
28.50°E
29.00°E
29.50°E

Fig. 1

Figure

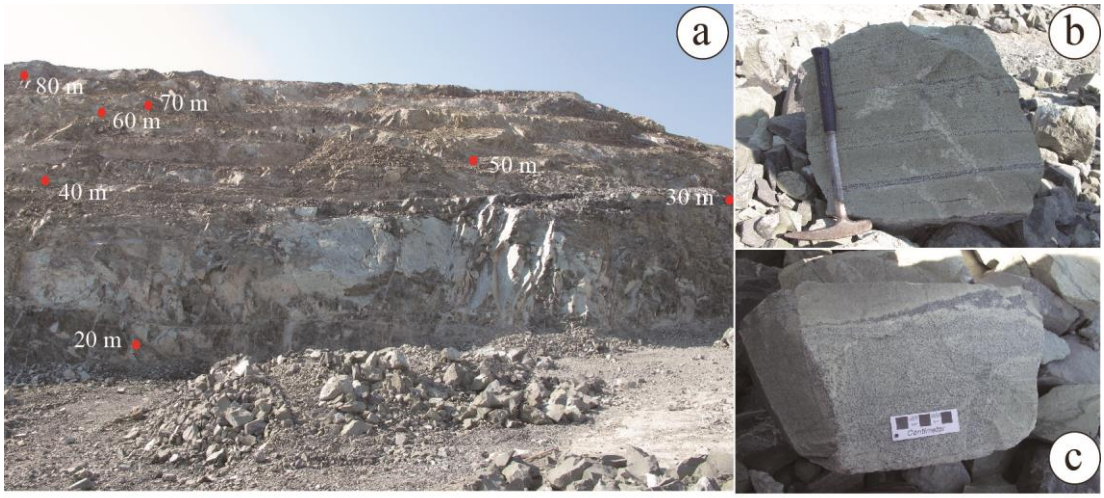

Fig. 2

Figure

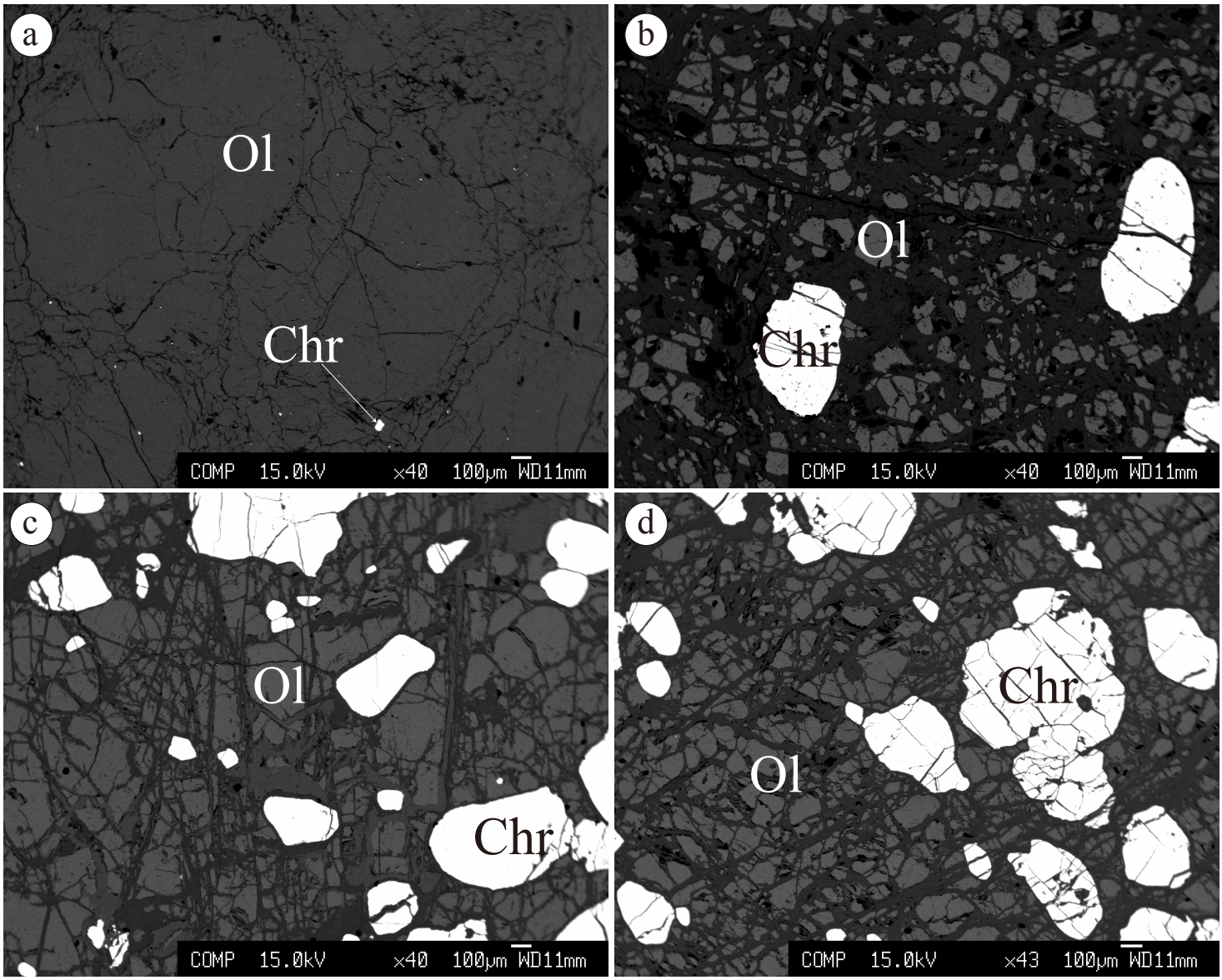
a
Ol
Chr
COMP 15.0kV ×40 100μm WD11mm
b
Ol
Chr
COMP 15.0kV ×40 100μm WD11mm
c
Ol
Chr
COMP 15.0kV ×40 100μm WD11mm
d
Chr
Ol
COMP 15.0kV ×43 100μm WD11mm

Fig. 3

Figure

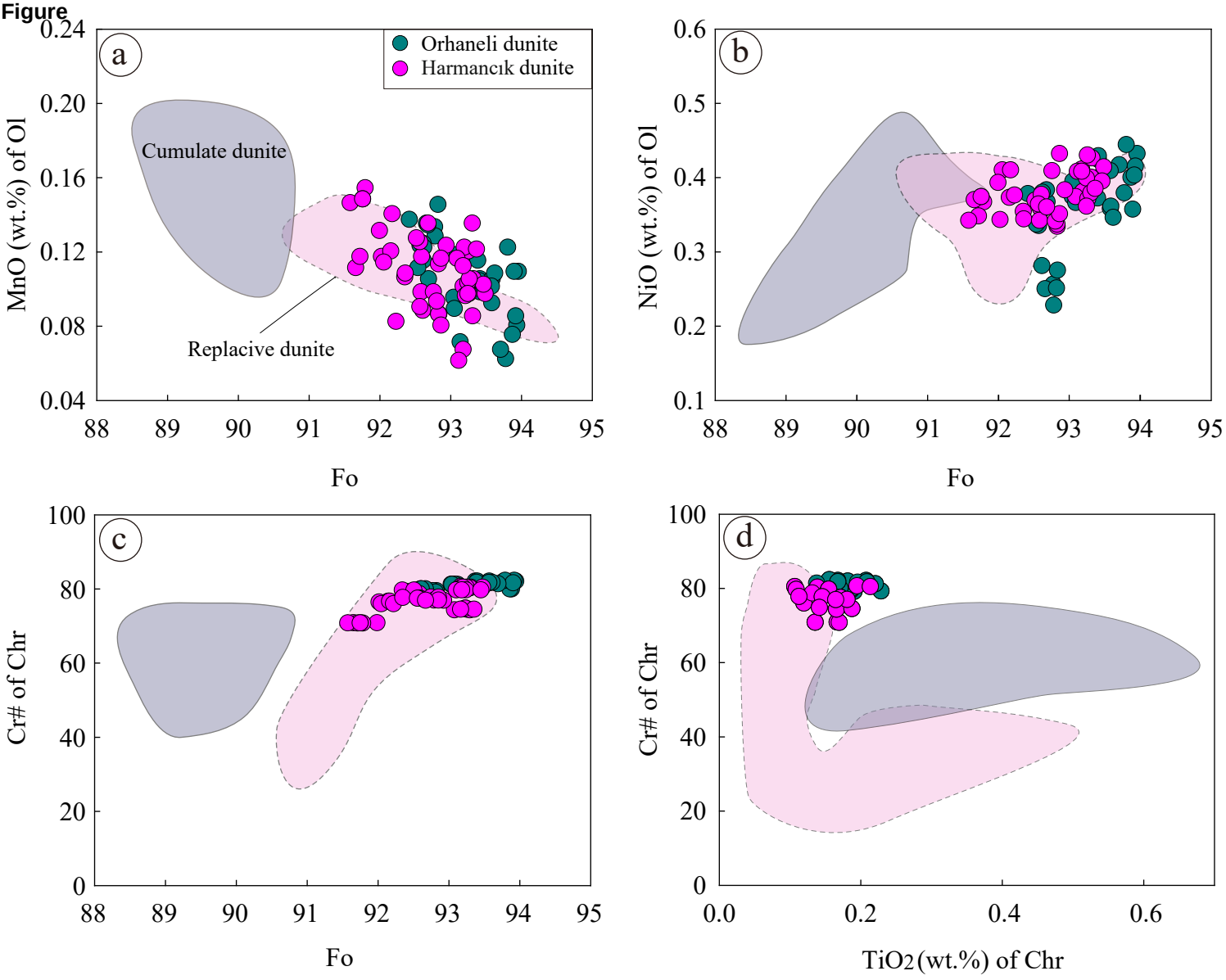
a
Orhaneli dunite
Harmancık dunite
Cumulate dunite
Replacive dunite
MnO (wt.%) of Ol
Fo
b
NiO (wt.%) of Ol
Fo
c
Cr# of Chr
Fo
d
Cr# of Chr
TiO2 (wt.%) of Chr

Fig. 4

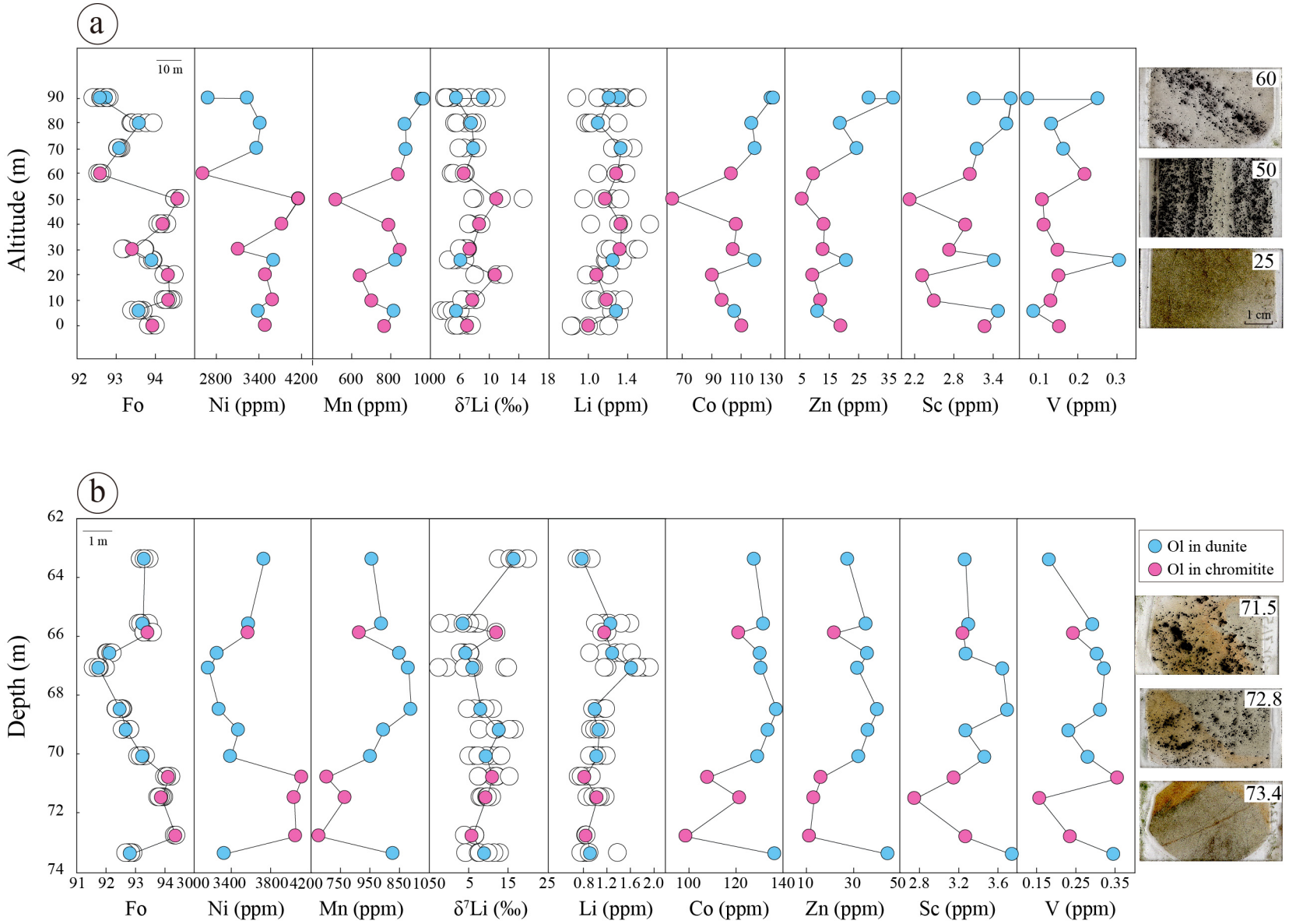
a
10 m
Altitude (m)
90
80
70
60
50
40
30
20
10
0
92 93 94
Fo
2800 3400 4200
Ni (ppm)
600 800 1000
Mn (ppm)
6 10 14 18
δ7Li (‰)
1.0 1.4
Li (ppm)
70 90 110 130
Co (ppm)
5 15 25 35
Zn (ppm)
2.2 2.8 3.4
Sc (ppm)
0.1 0.2 0.3
V (ppm)
60
50
25
1 cm
b
1 m
Depth (m)
62
64
66
68
70
72
74
91 92 93 94
Fo
3000 3400 3800 4200
Ni (ppm)
750 950 850 1050
Mn (ppm)
5 15 25
δ7Li (‰)
0.8 1.2 1.6 2.0
Li (ppm)
100 120 140
Co (ppm)
10 30 50
Zn (ppm)
2.8 3.2 3.6
Sc (ppm)
0.15 0.25 0.35
V (ppm)
Ol in dunite
Ol in chromitite
71.5
72.8
73.4

Fig. 5

Figure

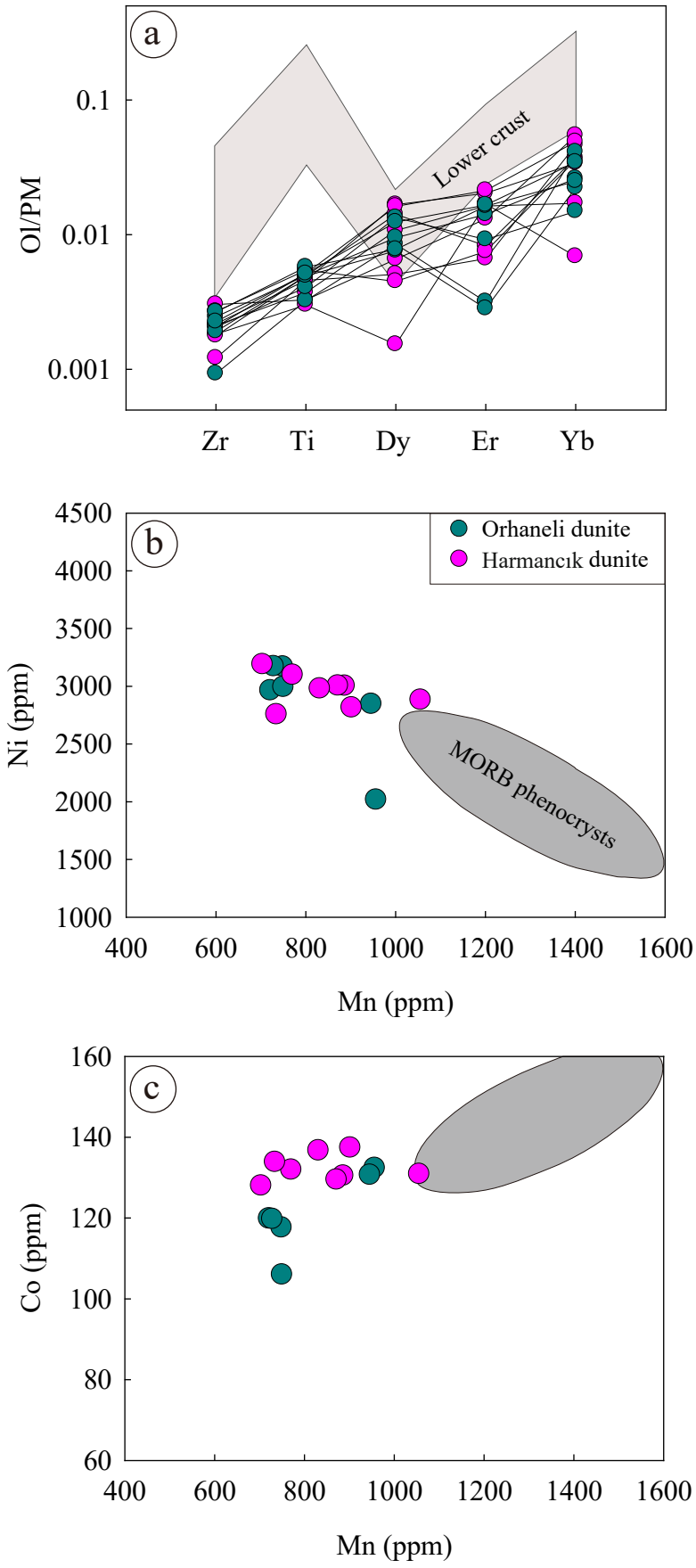
a
0.1
0.01
0.001
Ol/PM
Lower crust
Zr
Ti
Dy
Er
Yb
b
Orhaneli dunite
Harmancık dunite
MORB phenocrysts
Ni (ppm)
Mn (ppm)
c
Co (ppm)
Mn (ppm)

Fig. 6

Figure

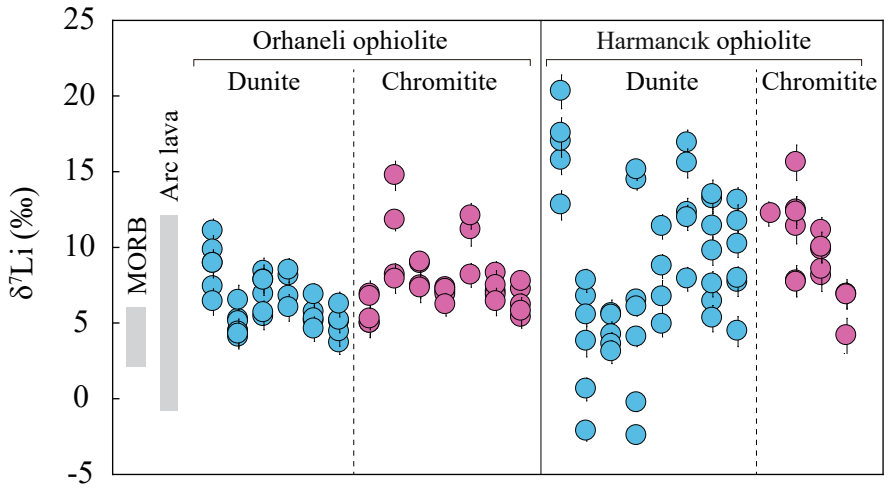
25
20
15
10
5
0
-5
δ7Li (‰)
MORB
Arc lava
Orhaneli ophiolite
Dunite
Chromitite
Harmancık ophiolite
Dunite
Chromitite

Fig. 7

Figure

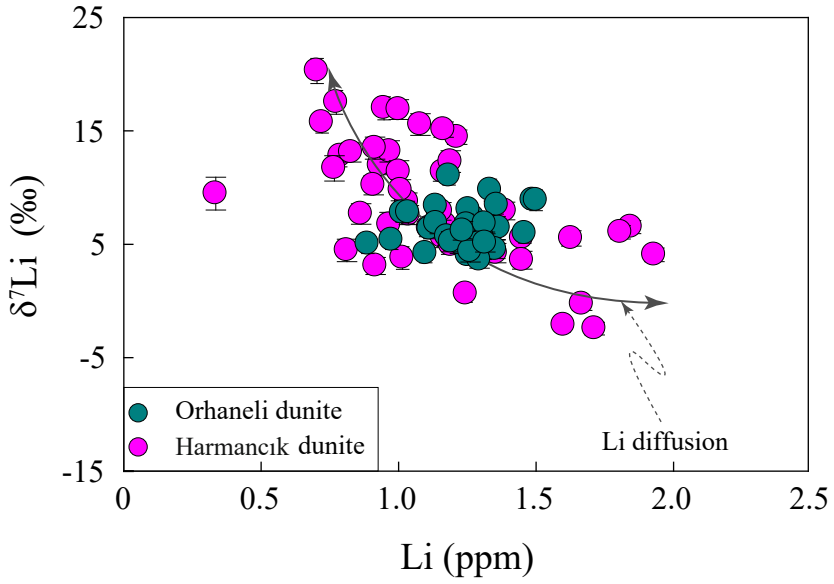
25
15
5
-5
-15
δ7Li (‰)
0
0.5
1.0
1.5
2.0
2.5
Li (ppm)
Orhaneli dunite
Harmancık dunite
Li diffusion

Fig. 8

Figure

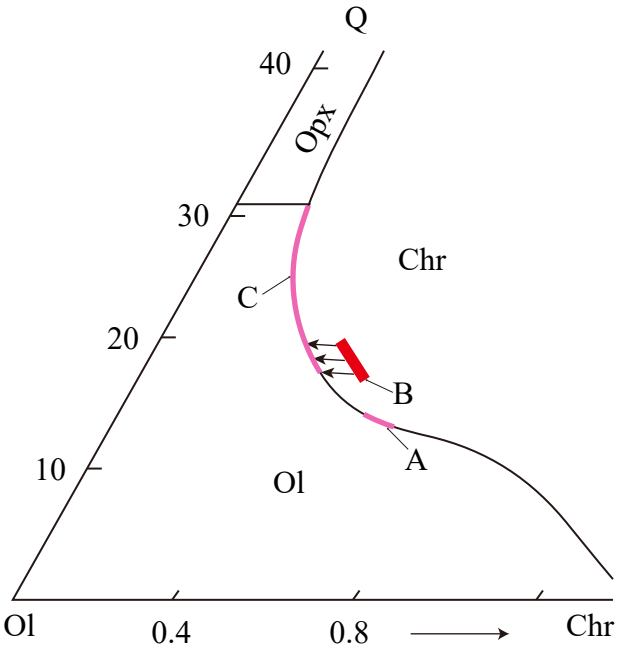

Fig. 9

Figure

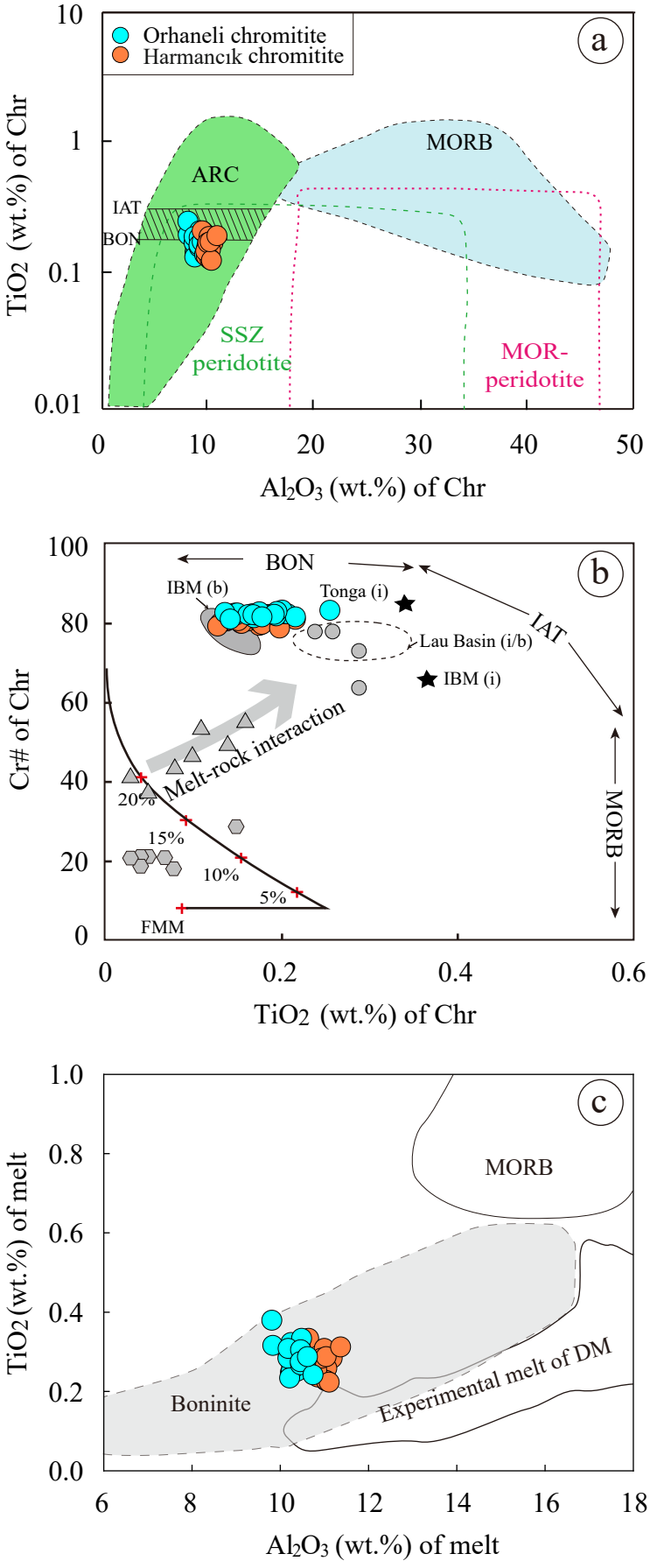

Fig. 10

Table
Click here to download Table: Table 1.docx

Table 1. Equilibrium temperature estimates for dunite and chromitite samples from the Orhaneli and Harmancık ophiolites

		T(Al-ol) [a]	T Ballhaus (°C) [b]
Orhaneli ophiolite			
90 m	Dunite	967	714
90 m	Dunite	960	724
80 m	Dunite	993	760
70 m	Dunite	974	778
25 m	Dunite	965	720
5 m	Dunite	973	754
average		**972**	**742**
60 m	Chromitite	977	754
50 m	Chromitite	982	828
40 m	Chromitite	971	779
30 m	Chromitite	973	863
20 m	Chromitite	969	840
10 m	Chromitite	982	839
0 m	Chromitite	973	940
average		**975**	**835**
Harmancık ophiolite			
63.4 m	Dunite	960	755
65.6 m	Dunite	979	719
66.6 m	Dunite	964	750
67.1 m	Dunite	937	691
68.5 m	Dunite	953	663
69.2 m	Dunite	966	682
70.1 m	Dunite	933	690
73.4 m	Dunite	972	724
average		**958**	**709**
65.9 m	Chromitite	985	767
70.8 m	Chromitite	984	858
71.5 m	Chromitite	1009	744
72.8 m	Chromitite	991	624
average		**992**	**748**

Supplementary material/Appendix (Files for online publication only)

Click here to download Supplementary material/Appendix (Files for online publication only): Data Repository.docx

*Declaration of Interest Statement

Conflicts of Interest Statement

Manuscript title: **Formation processes of dunites and chromitites in Orhaneli and Harmancık ophiolites (NW Turkey): evidence from in-situ Li isotopes and trace elements in olivine**

The authors whose names are listed immediately below certify that they have **No** affiliations with or involvement in any organization or entity with any financial interest (Such as honoraria; educational grants; participation in speakers' bureaus; membership, employment, consultancies, stock ownership, or other equity interest; and expert testimony or patent-licensing arrangements), or non-financial interest (such as personal or professional relationship, affiliations, knowledge or beliefs) in the subject matter or materials discussed in this manuscript.

Author names:
Chen Chen, Jan C.M. De Hoog, Ben-Xun Su, Jing Wang, İbrahim Uysal

The authors whose names listed immediately below report the following details of affiliation or involvement in an organization or entity with a financial or non-financial interest in the subject matter or materials discussed in this manuscript. Please specify the nature of the conflict on a separate sheet of paper if the space below is inadequate.

Author names:

This statement is signed by all the authors to indicate agreement that the above information is true and correct:

Author's name (typed)	Author's signature	Date
Chen Chen	Chen Chen	July. 24, 2020
Jan C.M. De Hoog		July. 24, 2020
Ben-Xun Su	Benxun Su	July. 24, 2020

Jing Wang	Jing Wang	July. 24, 2020
İbrahim Uysal		July. 24, 2020
Yan Xiao	Yan Xiao	July. 24, 2020